

# Fickian Insights Using Probability Theory as Logic

Peter E. Price, Jr.

LTD&G LLC, 4652 Vincent Avenue South, Minneapolis, MN 55410

---

## Abstract

In *Clearing Up Mysteries - The Original Goal* (Maximum Entropy and Bayesian Methods: Cambridge, England, 1988. Springer, pp. 1–27), Jaynes derived Fick’s Law for a dilute binary solution from Bayes’ Theorem by considering, probabilistically, the motion of dilute solute molecules. Modifying Jaynes’ prior, changing the frame of reference, and allowing for multicomponent systems, one can follow Jaynes’ logic to arrive at several expressions for the diffusion coefficient that are widely used in application to solvent-polymer systems. These results, however, do not generally satisfy required conditions over the full concentration range. This limitation is resolved by considering the joint motion of all components in the solution with the inclusion of known physical constraints. Doing so, one arrives at a new set of constitutive equations for binary and multicomponent diffusion that include Darken’s form as a limit and provide means to characterize inter-species correlations, removing the need for the *ad hoc* modifications of the thermodynamic term or substitution of bulk compositions with local compositions that have been proposed in the literature. In binary systems, the Bayesian expression for the mutual diffusion coefficient provides explicit limits on non-ideal mutual diffusion behavior, given component self-diffusion coefficients, that can be attributed to inter-species correlation versus stronger intra- and inter-species clustering. Applications of the model to published data for a set of binary systems are presented, along with pointers to further directions for research.

*Keywords:* mutual diffusion, self-diffusion, Bayesian, liquid mixture

---

## 1. Introduction

Fickian representations of diffusion describe component fluxes relative to a reference velocity as the products of mutual diffusion coefficients and gradients in some measure of concentration. For one dimensional molar diffusion in a binary system relative to the volume average velocity, Fick’s law has the form:

$$J_i^V = -D \frac{dC_i}{dx} \quad (1)$$

Based upon consideration of the correspondence between the Maxwell-Stefan (MS) and Fickian representations of diffusion, the Fickian mutual diffusion coefficients can be separated into the product of terms characterizing the frictional resistance to motion between diffusing entities,  $\mathcal{D}$ , and a thermodynamic correction factor,  $\Gamma$ . The thermodynamic factor is derived from the understanding that gradients in chemical potential, not concentration, are what drive diffusive fluxes [47, 29]:

$$D = \mathcal{D}\Gamma = \mathcal{D} \left( 1 + \frac{d \ln(\gamma_1)}{d \ln(x_1)} \right) \quad (2)$$

The literature contains a variety of approaches to constructing the frictional part from the constituent self-diffusion coefficients, many starting from Darken’s [13] binary form:

$$\mathcal{D} = x_1 D_2 + x_2 D_1 \quad (3)$$

where  $x_i$  are component mole fractions, and  $D_i$  are component self-diffusion coefficients.

Another line of expressions relating mutual and self-diffusion coefficients have followed from Vignes’ [50] empirical proposal:

$$\mathcal{D} = D_1^{x_2} D_2^{x_1} \quad (4)$$

The self-diffusion coefficients characterize the mean square displacements of species in a given time [15] in the absence of chemical potential gradients, and thus characterize the frictional resistance to motion of the individual components in a solution. Since self-diffusion coefficients are relatively easy to measure [35, 55], there is strong motivation to develop a robust theory relating mutual diffusion coefficients to constituent self-diffusion coefficients. Though tremendous progress has been made [1], elements of that progress remain linked to model forms that have found success through empirical modifications.

---

*Email address:* learningtodry@gmail.com (Peter E. Price, Jr.)

For example, recognition that there are often associations between components, both like and unlike, that can lead to cluster formation has led to modifications of both the frictional and the thermodynamic components in the mutual diffusion coefficient expressions. Several of these [8, 35] take the general form:

$$D = (x_1 D_2 + x_2 f D_1) \Gamma^\alpha \quad (5)$$

where  $f$  is a function [8] or constant [35] reflecting like-molecule polymerized clusters and  $\alpha$  ( $<1$ ) is a constant adapted from considerations of diffusion near consolute points [11, 36] to dampen the thermodynamic term. For modeling systems that include  $f$  across the full concentration range, concentration dependence in  $f$  is required for the model to reach the appropriate pure component limits.

Alternatively, several authors have shown improved agreement with experimental data by replacing the mole fractions in  $\mathbb{D}$  with local mole fractions [31, 54, 55] to account for molecular associations. However, as Jianmin et al. [26] note in regard to substitution of local for bulk compositions in binary models, multicomponent models based on local compositions must satisfy material balance constraints, Gibbs-Duhem consistency, and the Onsager reciprocal relations (ORR) to be broadly applicable. Substitution of local compositions for bulk values can lead to violations of these conditions.

Compilations of proposed expressions for binary mutual diffusion coefficients in terms of component self-diffusion coefficients have been presented by Hsu and Chen [23], Guevara-Carrion et al. [18], Obukhovskiy et al. [39], and most recently by Alabi-Babalola et al. [1]. All of these models are based on physical or empirical considerations of diffusion processes. By shifting perspective to an information theoretic viewpoint that incorporates prior physical knowledge, a new set of expressions for the relationship between self- and mutual diffusion coefficients can be derived for both binary and multicomponent systems. This approach follows and extends Jaynes' [24] use of probability theory as logic to derive Fick's law for a binary system from Bayes' Theorem. The resultant expressions provide new insights into existing theories and, since they satisfy required constraints, may well be useful in their own right.

Because this approach is very different from existing lines of development, we will limit our review of those existing lines to the above discussion and welcome the reader to consult the references. Below, we review Jaynes' derivation in more detail and show how several existing theories in common application for solvent-polymer systems [56, 2] follow from Jaynes' approach if we allow multiple components, alternative frames of reference, and, most importantly, if we recognize and include our prior information that chemical potentials drive the motion. The unifying aspect of these derivations is that they consider only information about a single species. Failure to put constraints on the joint movements in multicomponent systems results in expressions that satisfy the ORR only under special conditions [41]. The present approach sheds new light on the information content of these existing theories and points the way to further development. By considering the joint information in a binary system, we extend Jaynes' binary results to a new expression for the mutual diffusion coefficient that includes the self-diffusion coefficients of both components and a function that accounts for correlated motion of the components. To understand the range of possibilities for this model, we compare its results relative to several other theories for some nonphysical parameter sets, and then examine its performance relative to a sample of published experimental data. Finally, we extend the joint information derivation to multicomponent systems and provide a comparison for a ternary system to the multicomponent form of Darken's equation [41] derived from Bearman's [6] friction-based approach.

Hopefully the reader, like Jaynes, will find excitement and opportunity in failure, because the Bayesian model, while showing insightful success for some systems, shows spectacular failure in others. In many cases, the failure may be due to our own failure to account for uncertainty in the underlying characterization of a given system's self-diffusion and thermodynamic behavior. In other cases, the failure signal is robust and attributable to omission of relevant physical information in the theory, appearing when strong clustering is expected. In that sense, the model delineates behavior that can be explained by increased friction, and hence correlation structure, in the self-diffusion motions from that which requires more complete accounting of cluster formation.

## 2. Probability and Bayes' Theorem

Probability is a concept that has a variety of interpretations [22], and its foundations have been rife with controversies, both philosophical and mathematical. Because Jaynes' results are extended here, his framework for probability [25] will be followed without further justification. To wit, the probability  $P(x | I)$  of a proposition  $x$  is taken to represent degree of belief in  $x$  given one's specified or assumed state of knowledge about the problem at hand,  $I$ , on a scale of real numbers spanning from  $P(x | I) = 0$  when  $x$  is known to be false to  $P(x | I) = 1$  when  $x$  is known to be true. Elements to the right of the vertical line in this notation are taken to be true. The probabilities of all mutually exclusive propositions must sum to 1. Calculations with probabilities rely on the product rule for joint propositions:

$$P(x, y | I) = P(x | I) P(y | x, I) = P(y | I) P(x | y, I) \quad (6)$$

And the sum rule for a proposition  $x$  and its negation  $\bar{x}$ :

$$P(x | I) + P(\bar{x} | I) = 1 \quad (7)$$

Bayes' Theorem is a logical outcome of these rules, and for many practical applications in the physical sciences including the application described below, takes the form:

$$P(h | d, I) = \frac{P(h | I) P(d | h, I)}{P(d | I)} \quad (8)$$

where  $h$  is represents a hypothesis, and  $d$  represents the data. The term on the left is the posterior probability of hypothesis  $h$  given data  $d$  and other information in the problem formulation,  $I$ . The first term in the numerator on the right is the prior probability for hypothesis  $h$ . Priors incorporate information regarding  $h$  available or assumed before learning from data. If one begins an inference from a different state of information, one's prior may change, leading to a different posterior. The second term in the numerator on the right is the likelihood of the data  $d$  given hypothesis  $h$ . The denominator on the right is referred to as the evidence for data  $d$  and serves as a normalizing constant for the posterior.

### 3. Inference on Individual Component Motions

#### 3.1. Jaynes' Derivation of Fick's Law for a Binary System from Bayes' Theorem

Jaynes [24] considered a solution of sugar in water "so dilute that each sugar molecule interacts constantly with the surrounding water, but almost never encounters another sugar molecule." Given a nonuniform concentration profile in one dimension, he wrote the species conservation law for sugar and then, without stating so explicitly, expressed the flux as Fick's Law relative to the volume average velocity:

$$J_1^V = -D \frac{dC_1}{dx} \quad (9)$$

where  $C_1$  is the sugar concentration, and  $J_1^V$  is the diffusive flux of sugar,  $D$  is the mutual diffusion coefficient. The form of Jaynes' conservation equation implies an assumption that the volume average velocity was zero. Jaynes also made no stated consideration of hydration, an issue of importance to the sugar-water system he chose for illustrative purposes and related to various theories of cluster diffusion mentioned above.

Fick (republished [16]) proposed a molecular diffusive flux relation based upon the gradient of concentration. He did so on phenomenological grounds, by analogy to Fourier's and Ohm's Laws for the diffusion of thermal energy and electricity, respectively. Jaynes sought a more fundamental basis for this expression and began by writing a centered difference expression for the velocity,  $v$ , of a molecule of sugar presently located at position  $x(t)$ :

$$v = \frac{x(t + \tau) - x(t - \tau)}{2\tau} = \frac{y - z}{2\tau} \quad (10)$$

The averaging time,  $\tau$ , is assumed long with respect to the time scale of the rapid thermal fluctuations of the molecules in solution. Next, noting that movement of the sugar molecule in the dilute solution is the result of many small collisions, primarily between the sugar molecule and surrounding water, Jaynes invoked the Central Limit Theorem to give a Gaussian probability distribution for the future location of a molecule,  $y = x(t + \tau)$ , given its present position,  $x(t)$ :

$$P(y | x, \tau, I) = A_1 \exp \left[ -\frac{(y - x)^2}{2(\sigma(\tau))^2} \right] \quad (11)$$

where " $I$  stands for the general prior information stated or implied in our formulation of the problem" [24], and  $A_1$  is a normalizing constant. The "spreading function,"  $(\sigma(\tau))^2$ , is the expected square of the molecule's displacement in time  $\tau$ ,  $(\sigma(\tau))^2 = (\delta x)^2$ . The probability distribution in Eq. (11) is symmetric about the present position of the molecule, and so the expected and most probable values of  $y$  are just the current position. Jaynes noted that the time-reversal invariance of the equations of motion suggests that the same form should hold for the past position of the molecule,  $z = x(t - \tau)$ . This implies that the expected velocity of the molecule, Eq. (10), should be zero. The fact that gradients in such a dilute system do level out with time indicates that average velocities are not zero, presenting an apparent paradox. Jaynes addressed this apparent paradox by noting that, "The equations of motion are symmetric in past and future, but our information about the particles is not" [24]. Our information about the past concentration profile is what breaks the symmetry of the predicted movement. He then wrote Bayes' Theorem for the probability distribution of past location,  $z$ , of the sugar molecule given its present position,  $x$ , the time step,  $\tau$ , and the rest of our prior information,  $I$ :

$$P(z | x, \tau, I) = A_2 P(z | \tau, I) P(x | z, \tau, I) \quad (12)$$

where, again,  $A_2$  is a normalizing constant, the inverse of the evidence,  $P(x | \tau, I)$ . Replacing  $y$  with  $x$  and  $x$  with  $z$ , Eq. (11) also represents the probability distribution for the present molecule position, given its past position, taken over the class of all motions allowed by the stated or implied molecular dynamics,  $P(x | z, \tau, I)$ . It is our prior knowledge of the concentration

field that restricts the possible motions within this class. Thus, Jaynes stated that the prior probability of the molecule's position,  $P(z | \tau, I)$ , is "clearly proportional to  $C_1(z)$ ." Inserting these equations into Eq. (12) and taking the logarithm gives:

$$\ln(P(z | x, \tau, I)) = \ln(A_2) + \ln(C_1(z)) - \frac{(x-z)^2}{2(\sigma(\tau))^2} \quad (13)$$

The most probable past position of the molecule now at  $x$  is found by differentiating with respect to  $z$  and setting the result equal to zero. Solving the resulting equation for the most probable past position of the molecule gives:

$$\hat{z} = x + (\sigma(\tau))^2 \frac{d \ln(C_1(z))}{dz} = x + (\delta x)^2 \frac{d \ln(C_1)}{dz} \quad (14)$$

Jaynes appears to have assumed that the gradient term, evaluated at time  $\tau$  in the past and location  $\hat{z}$ , was sufficiently close to its present value at  $x$  to substitute this result into Eq. (10) to write the most probable drift velocity as:

$$\hat{v} = -\frac{(\delta x)^2}{2\tau} \frac{d \ln(C_1)}{dx} \quad (15)$$

This leads to the flux expression:

$$J_1^V = C_1 \hat{v} = -\frac{(\delta x)^2}{2\tau} \frac{dC_1}{dx} = -D_1 \frac{dC_1}{dx} = -D \frac{dC_1}{dx} \quad (16)$$

The interested reader will find much more to contemplate in Jaynes' [24] discussion, but we note that the mutual diffusion coefficient,  $D$ , is the self-diffusion coefficient of the sugar in the dilute solution,  $D_1$ , defined in terms of a sugar molecule's expected square displacement in time. This is Einstein's expression for the (tracer or self-) diffusion coefficient in Brownian motion (reprinted Einstein et al. [15]). While one may take exception to any of Jaynes' assumptions, since Bayes' Theorem is a consequence of the product and sum rules of probability, Fick's Law and Einstein's expression for  $D$  are consistent outcomes of applying probability theory as logic given the stated assumptions. Eq. (16) is also consistent with the fundamental result that in the dilute limit, the mutual diffusion coefficient in a binary system approaches the self-diffusion coefficient of the dilute component.

### 3.2. Fick's Law from the Mean

Rather than considering only the most probable past position of a molecule, we can derive the expected (mean) location by linearizing the concentration-based prior about the current position, which we take as  $x = 0$ :

$$P(z | x = 0, \tau, I) = A_3 \left( C_{1,x=0} + \frac{dC_1}{dx} \Big|_{x=0} z \right) \exp \left[ -\frac{z^2}{2(\sigma(\tau))^2} \right] \quad (17)$$

$A_3$  is a constant. Again, the gradient is assumed constant on the time scale of interest. If we treat the domain as infinite, then far from the current position,  $x = 0$ , any non-zero gradient in the linearized concentration prior will lead to invalid negative probabilities. However, we proceed on the assumption that the likelihood function decays much faster than the gradient term and renders such errors negligible for present purposes. The normalizing factor is given by the integral:

$$P(x = 0 | \tau, I) = \int_{-\infty}^{\infty} A_3 \left( C_{1,x=0} + \frac{dC_1}{dx} \Big|_{x=0} z \right) \exp \left[ -\frac{z^2}{4\tau D_1} \right] dz = \sqrt{4\pi\tau D_1} A_3 C_{1,x=0} \quad (18)$$

And the expected (mean) past position of the molecule now at  $x = 0$  is:

$$\langle z \rangle = \int_{-\infty}^{\infty} \frac{z \left( C_{1,x=0} + \frac{dC_1}{dx} \Big|_{x=0} z \right) \exp \left[ -\frac{z^2}{4\tau D_1} \right] dz}{\sqrt{4\pi\tau D_1} C_{1,x=0}} = \frac{2\tau D_1}{C_{1,x=0}} \frac{dC_1}{dx} \Big|_{x=0} \quad (19)$$

This leads, once again, to Fick's Law:

$$J_1^V = C_1 \langle v \rangle = C_1 \frac{-\langle z \rangle}{2\tau} = -D_1 \frac{dC_1}{dx} \Big|_{x=0} = -D \frac{dC_1}{dx} \quad (20)$$

### 3.3. Multiple Components, Alternative Reference Frames, and a Potential Prior

Jaynes' reasoning is based on consideration of a single molecule, but the resultant expression is commonly applied in a continuum context. In the spirit of investigation, we proceed allowing the continuum concept of species coexistence in space while continuing to construct expectations about individual component motions. Under such an assumption, the logic of Jaynes' derivation does not change if there are multiple dilute components. Nor does it change if the molecular motions occur relative to a moving frame of reference. Finally, diffusion does not have to occur down a concentration gradient [29]. Fundamentally, diffusive motions occur from regions of higher chemical potential to regions of lower chemical potential. This is prior information that can be readily incorporated into Bayes' Theorem by replacing Jaynes' concentration-based past-position prior with one based on component activity.

In a reference frame moving with velocity  $v^{ref}$ , the mapping between the moving coordinate,  $x$ , and the laboratory coordinate,  $x^{lab}$ , is:

$$x^{lab} = x + v^{ref}t \quad (21)$$

The position of a molecule of component  $i$ , presently at the origin of the moving frame ( $x_i = 0$  at  $t = 0$ ), after time  $t = \tau$  is then:

$$x_i(\tau) = (v_i - v^{ref})\tau \quad (22)$$

where  $v_i$  is the particle velocity in the laboratory frame.

With respect to the moving reference frame, the species velocity, centered at the present position and time ( $x_i = 0$  and  $t = 0$ ), retains a form similar to Eq. (10):

$$v_i - v^{ref} = \frac{x_i(\tau) - x_i(-\tau)}{2\tau} = \frac{y_i - z_i}{2\tau} = \frac{-z_i}{2\tau} \quad (23)$$

where  $y_i$  and  $z_i$  are the future and past particle positions of component  $i$  in the moving frame of reference. If the reference velocity represents some bulk translation of the components in such a way that the molecular collisions can be considered as superimposed on the motion described by the reference velocity, then Eq. (11) will continue to hold for the future position of a molecule of component  $i$  in the moving reference frame. Under such conditions, the expected future position of the molecule of  $i$ ,  $y_i$ , is just its present position, resulting in the last expression for the species velocity given in Eq. (23).

The results that follow can also be derived by considering the expected behavior using a linearization of the component activity about the current position, analogous to the results in Section 3.2.

#### 3.3.1. Zielinski and Hanley's Model

Consider, for example, mutual diffusion of a molecule of species  $i$  relative to the mass average velocity,  $v^{ref} = v^m$ , of the system. Recognizing that a molecule at some current position is more likely to have come from a location of higher chemical potential in time past, and letting species activity serve as a measure of that potential, we replace Jaynes' concentration-based prior with a prior probability for the past position of that molecule proportional to its activity,  $a_i$ . It is straightforward to follow Jaynes' derivation to arrive at the most probable past position:

$$\hat{z}_i = x_i + (\sigma_i(\tau))^2 \frac{d \ln(a_i(z))}{dz} = x_i + (\delta x_i)^2 \frac{d \ln(a_i(z))}{dz} \quad (24)$$

Following the earlier results, the most probable species velocity relative to the reference velocity becomes:

$$\hat{v}_i - v^m = -\frac{(\delta x_i)^2}{2\tau} \frac{d \ln(a_i)}{dx} \quad (25)$$

The corresponding mass diffusion flux relative to the mass average velocity is:

$$j_i = \rho_i (\hat{v}_i - v^m) = -D_i \rho_i \frac{d \ln(a_i)}{dx} \quad (26)$$

where  $D_i$  is the component  $i$  self-diffusion coefficient. For multicomponent systems, the gradient term can be expanded in the component concentrations using the chain rule. We can map the corresponding species mass flux to the volume average reference frame [19] using the relation:

$$j_i^V = j_i - \rho_i \sum_{k=1}^N \hat{V}_k j_k = \left(1 - \rho_i (\hat{V}_i - \hat{V}_N)\right) j_i - \rho_i \sum_{k=1}^{N-1} (\hat{V}_k - \hat{V}_N) j_k \quad (27)$$

where the  $\hat{V}_k$  are the species partial specific volumes. Substituting Eq. (26) into this expression gives the diffusion model presented for ternary systems by Zielinski and Hanley [56]. The same model can be developed in the Bearman [6] friction factor framework by assuming that the friction factors are inversely proportional to the component molecular weights.

The literature contains some discussion of the Gibbs-Duhem consistency of this model and its importance in satisfying material balance constraints [56, 38, 41]. A related and detailed examination of restrictions on friction factors imposed by both the entropy inequality and the Gibbs-Duhem equation was presented by Vrentas and Vrentas [51]. For the mass average reference frame, the component mutual diffusion fluxes are constrained to satisfy the summation rule:

$$\sum_{k=1}^N j_k = \sum_{k=1}^N D_k \rho_k \frac{\partial \ln(a_k)}{\partial x} = 0 \quad (28)$$

and the isobaric, isothermal Gibbs-Duhem equation is:

$$\sum_{k=1}^N \frac{\rho_k}{M_k} \frac{\partial \mu_k}{\partial x} = \sum_{k=1}^N \frac{\rho_k}{M_k} \frac{\partial \ln(a_k)}{\partial x} = 0 \quad (29)$$

One can see by inspection that Gibbs-Duhem consistency requires that all of the component self-diffusion coefficients,  $D_i$ , be inversely proportional to the molecular weights:

$$D_i \propto \frac{1}{M_i} \quad (30)$$

Such self-diffusion behavior is not typical. Our inferential derivation of this mutual diffusion model, however, made no use of the Gibbs-Duhem relationship. Because our inference is optimal in the Bayesian sense given the assumptions described above, the present derivation may help explain why Zielinski and Hanley's model performs so well up to moderate solvent concentrations even in instances where the self-diffusion coefficients do not satisfy the Gibbs-Duhem consistency constraints. Likewise, the fact that we did not use any information about the other species in the system of interest, and thus imposed no a priori constraints on the individual species fluxes, explains why failures of the theory occur when the proportionality constraint is not met.

### 3.3.2. Alloy and Duda's Model

It is also a straightforward exercise to follow this same logic using the volume average velocity as the reference velocity. This leads to the following expression for the mass diffusion flux of component  $i$ :

$$j_i^V = \rho_i (\hat{v}_i - v^V) = -D_i \rho_i \frac{d \ln(a_i)}{dx} \quad (31)$$

This model was shown for ternary systems as Case 4 in the work of Alsoy and Duda [2] and is the model derived using Bearman's [6] friction-factor approach by assuming that the friction factors are inversely proportional to the component partial molar specific volumes. Consideration of the Gibbs-Duhem consistency of this model also requires that the self-diffusion coefficients,  $D_i$ , be inversely proportional to the component specific volumes.

$$D_i \propto \frac{1}{\hat{V}_i} \quad (32)$$

Again, however, the model often performs quite well even when the self-diffusion coefficients do not satisfy this constraint, suggesting that its inferential basis helps explain why it is more broadly applicable than might be expected from its mechanical foundations.

## 4. Joint Inference on All Component Motions

The problems that concern us in diffusion theory involve systems with more than one component, and yet the derivations above used only information about single components. By allowing the concept of species superposition, we can now consider the problem of mutual diffusion as one of inference on the joint probability distribution of past positions for molecules of all species that are presently at the position of interest.

### 4.1. Binary Systems

Let us consider the situation in a binary system where molecules of components 1 and 2 are presently centered at the origin ( $x_i = 0$  and  $t = 0$ ) of a frame of reference moving with velocity  $v^{ref}$ . As above, if the reference velocity represents some bulk translation of the components in such a way that the molecular collisions can be considered as superimposed on the motion described by the reference velocity, then Eq. (11) will continue to hold for the future position of a molecule of component  $i$  in the moving reference frame. Jaynes' derivation considered a very dilute solution. In situations where the components are not dilute but the gradients are not extreme, the neighborhood of any molecule of interest on the relevant scales of time and space can be assumed constant, collisions between like and unlike molecules locally symmetric, and thus the

Central Limit Theorem still applicable. Let us further assume that inter-molecular forces may result in associations between molecules of different species, and thus in correlations between the local movements of those molecules. Such associations form the conceptual foundation of local composition theories, e. g., Renon and Prausnitz [42]. Assuming probabilities of prior positions are proportional to the species' activities, then the joint posterior distribution for the position of the molecules of species 1 and 2, presently at the origin of the moving reference frame, at time  $\tau$  in the past is:

$$P(z_1, z_2 | x_1 = 0, x_2 = 0, \tau, I) = A_4 (a_1(z_1)) (a_2(z_2)) \exp \left[ -\frac{\mathbf{z}^T \boldsymbol{\Sigma}^{-1} \mathbf{z}}{2} \right] \quad (33)$$

$$\mathbf{z} = \begin{bmatrix} z_1 \\ z_2 \end{bmatrix}, \boldsymbol{\Sigma} = \begin{bmatrix} (\sigma_1(\tau))^2 & r_{12} \sigma_1(\tau) \sigma_2(\tau) \\ r_{12} \sigma_1(\tau) \sigma_2(\tau) & (\sigma_2(\tau))^2 \end{bmatrix}$$

where  $A_4$  is a normalizing constant, and  $r_{12}$  is the correlation coefficient for the motions of the two components.

Before proceeding, we will invoke and generalize our earlier connection between the spreading functions,  $(\sigma_1(\tau))^2$ , and the component self-diffusion coefficients,  $D_i$ . That is, we assume that the spreading functions are locally constant for the time and space scales of interest and that a more complete description of the local self-diffusion behavior in a given state is described by the covariance matrix in the above likelihood function:

$$\boldsymbol{\Sigma} = \begin{bmatrix} \tau D_1 & \tau r_{12} \sqrt{D_1 D_2} \\ \tau r_{12} \sqrt{D_1 D_2} & \tau D_2 \end{bmatrix} \quad (34)$$

If we invert this covariance matrix, expand the terms in the exponential, and take the logarithm of the resultant expression, we find:

$$\ln(P(z_1, z_2 | x_1 = 0, x_2 = 0, \tau, I)) = \ln(A_4) + \ln(a_1(z_1)) + \ln(a_2(z_2)) - \frac{z_1^2 D_2 + 2z_1 z_2 r_{12} \sqrt{D_1 D_2} + z_2^2 D_1}{4\tau D_1 D_2 (1 - r_{12}^2)} \quad (35)$$

Recognizing this is not the usual sequence of operations, see Section 4.1.1, it is useful to consider what additional prior information we might want to include before continuing our analysis. In many applications, a particular reference frame is chosen to simplify the final species continuity equations. Furthermore, it is desirable to have the resultant theory satisfy the Gibbs-Duhem relation. Consider molar diffusion with respect to the volume average velocity, where activities satisfy the Gibbs-Duhem relation. The isothermal, isobaric Gibbs-Duhem relation requires:

$$C_1 \frac{d \ln(a_1)}{dz} + C_2 \frac{d \ln(a_2)}{dz} = 0 \quad (36)$$

or

$$\frac{d \ln(a_2)}{dz} = -\frac{\phi_1 \tilde{V}_2}{\phi_2 \tilde{V}_1} \frac{d \ln(a_1)}{dz} \quad (37)$$

where  $\phi_i$  are species volume fractions, and  $\tilde{V}_i$  are species partial molar specific volumes.

For molar diffusion with respect to the volume average velocity, we have the following relationship between species fluxes about the present point of interest:

$$\tilde{V}_1 J_1 + \tilde{V}_2 J_2 = \tilde{V}_1 C_1 (v_1 - v^V) + \tilde{V}_2 C_2 (v_2 - v^V) = 0 \quad (38)$$

We expect these relations to hold on average at a macroscopic scale, but we are focused on inferences about particular molecules at a particular location and time. Again, in the spirit of investigation, let us assume that we can use this relation to further restrict the allowable motions of our molecules, which are presently at the origin of our reference frame:

$$\tilde{V}_1 J_1 + \tilde{V}_2 J_2 = \phi_1 \frac{0 - z_1}{2\tau} + \phi_2 \frac{0 - z_2}{2\tau} = 0 \quad (39)$$

Thus:

$$z_2 = -\frac{\phi_1}{\phi_2} z_1 \quad (40)$$

Eq. (40) constrains the allowable class of component 2 motions relative to those of component 1. Under this constraint, the most probable past position of component 2 is determined by the most probable past position of component 1. Differentiating Eq. (35) with respect to  $z_1$ , recognizing  $z_2 = f(z_1)$ , and then using Eq. (37) and Eq. (40) with the assumption that the activity gradients are constant in the  $(z_1, z_2)$  neighborhood of the point of interest over the relevant time scale gives:

$$\begin{aligned} \frac{d \ln(a_1(z_1))}{dz_1} + \frac{d \ln(a_2(z_2))}{dz_2} \frac{dz_2}{dz_1} - \frac{\partial}{\partial z_1} \left( \frac{z_1^2 D_2 + 2z_1 z_2 r_{12} \sqrt{D_1 D_2} + z_2^2 D_1}{4\tau D_1 D_2 (1-r_{12}^2)} \right) = \\ \left( 1 + \frac{\phi_1^2 \tilde{V}_2}{\phi_2^2 \tilde{V}_1} \right) \frac{d \ln(a_1(z_1))}{dz_1} - z_1 \left( \frac{\phi_2^2 D_2 + 2\phi_1 \phi_2 r_{12} \sqrt{D_1 D_2} + \phi_1^2 D_1}{2\tau \phi_2^2 D_1 D_2 (1-r_{12}^2)} \right) = 0 \end{aligned} \quad (41)$$

Thus:

$$J_1^V = C_1 (\hat{v}_1 - v^V) = C_1 \frac{-z_1}{2\tau} = -D \frac{dC_1}{dx} \quad (42)$$

where:

$$D = \frac{D_1 D_2 (1 - r_{12}^2)}{\phi_1^2 D_1 + 2\phi_1 \phi_2 r_{12} \sqrt{D_1 D_2} + \phi_2^2 D_2} \left( \phi_2^2 + \phi_1^2 \frac{\tilde{V}_2}{\tilde{V}_1} \right) \frac{d \ln(a_1)}{d \ln(C_1)} \quad (43)$$

Or in the usual form:

$$D = \frac{D_1 D_2 (1 - r_{12}^2)}{\phi_1^2 D_1 + 2\phi_1 \phi_2 r_{12} \sqrt{D_1 D_2} + \phi_2^2 D_2} \left( \phi_2^2 + \phi_1^2 \frac{\tilde{V}_2}{\tilde{V}_1} \right) \left( \frac{x_1 \tilde{V}_1 + x_2 \tilde{V}_2}{\tilde{V}_2} \right) \Gamma \quad (44)$$

This is an information theoretic expression, based on the assumptions described above, relating the Fickian mutual diffusion coefficient for a binary system to the component self-diffusion coefficients. Here we see that probability theory applied as logic provides a truly “physics informed” inference engine. To satisfy the required condition that the mutual diffusion coefficient approach the dilute component self-diffusion coefficients in the pure component limits, the correlation coefficient,  $r_{12}$ , must also be a function of concentration that approaches zero in the pure component limits. Otherwise, the theory offers no fundamental form for  $r_{12}$ , leaving it open for further investigation. This is not unlike the characterization of clustering in Carman [8], where the concentration dependent clustering function must be determined independently. In keeping with the usual notion of “ideal” behavior occurring when component molecular motions are independent, we can define ideal systems as having component movements uncorrelated across the concentration range,  $r_{12} = 0$ .

Given measured self- and mutual diffusion coefficients at equivalent concentrations, or some functional representation thereof, Eq. (44) can be rearranged into a quadratic equation for  $r_{12}$ . For the systems we have examined, we find either two real solutions for  $r_{12}$ , a lesser root that is always less than or equal to zero and a greater root that can be either negative or positive, or no real solution. Rearranging Eq. (44) into quadratic form in  $r_{12}$ , we find two conditions for real roots:

$$D_1 \left( \phi_2^2 + \phi_1^2 \frac{\tilde{V}_2}{\tilde{V}_1} \right) \left( \frac{x_1 \tilde{V}_1 + x_2 \tilde{V}_2}{\tilde{V}_2} \right) \Gamma - D_m \phi_2^2 \geq 0 \quad (45)$$

and

$$D_2 \left( \phi_2^2 + \phi_1^2 \frac{\tilde{V}_2}{\tilde{V}_1} \right) \left( \frac{x_1 \tilde{V}_1 + x_2 \tilde{V}_2}{\tilde{V}_2} \right) \Gamma - D_m \phi_1^2 \geq 0 \quad (46)$$

With regard to ideal behavior, the greater root is always zero when the mutual is constructed from the Darken form and the self-diffusion coefficients are inversely proportional to their associated molar volumes. Of course, one could have ideal behavior in the Bayesian model sense,  $r_{12} = 0$ , even when the self-diffusion coefficients are not inversely proportional to their associated molar volumes, and the model would generate mutual diffusion coefficients that differ from the “ideal” Darken values. When there is no real solution, the model is indicating either errant measurements; inconsistent characterization of diffusion and/or thermodynamic behavior; or some other missing physics, e. g., clustering, in the model. Lack of a real solution is a failure mode that should spark further research. In the systems examined below, we observe such failure when strong clustering is known or expected to occur. As we will see below, the model fails to give real roots for  $r_{12}$  in several systems in which strong clustering is not expected. These failures are not fundamental insofar as taking a Bayesian viewpoint of the uncertainty in our representations of both diffusion coefficients and component activities allows descriptions with real roots for  $r_{12}$  to be found.

#### 4.1.1. Incorporating the Flux Constraint as Prior Information

As stated above, the flux constraint, Eq. (39), should be incorporated into the probability distribution as a constraint on expectations, not as a hard constraint on individual molecular motions. This can be done using the Maximum Entropy procedure [9]. The challenge in this approach is that the resultant form of the probability distribution for the past positions of molecules becomes unwieldy, rendering concise expressions of the mutual diffusion coefficients, like Eq. (44), unavailable. We reserve this line of inquiry for future investigation.



### 4.1.2. Comparison with Some Existing Theories

To understand what constraints are imposed by their algebraic forms, we examine the behavior of various models for the MS diffusion coefficients,  $\mathcal{D}$ , in dimensionless terms, for some simplified systems with constant self-diffusion coefficients. By removing the nonlinearities associated with the concentration dependent behavior prevalent in real systems, we can develop a clearer understanding of the constraints imposed by the various model forms.

In the first case, shown in Fig. 1(a), the two components have identical molecular weights and molar volumes but the component 2 self-diffusion coefficient is 10% greater than that of component 1. The Darken coefficients vary linearly across the concentration range. The Vignes coefficients deviate below the Darken values only slightly. The Bayesian model values, however, display a sigmoidal shape across the concentration range that deviate below and above the Darken values and approach the pure component limits tangentially to the dilute component self-diffusion values. Tangential approach of the frictional term to the self-diffusion coefficients and sigmoidal deviations from the Darken coefficients are both behaviors that could potentially be investigated experimentally in an ideal system and appears to be unique to the Bayesian model.

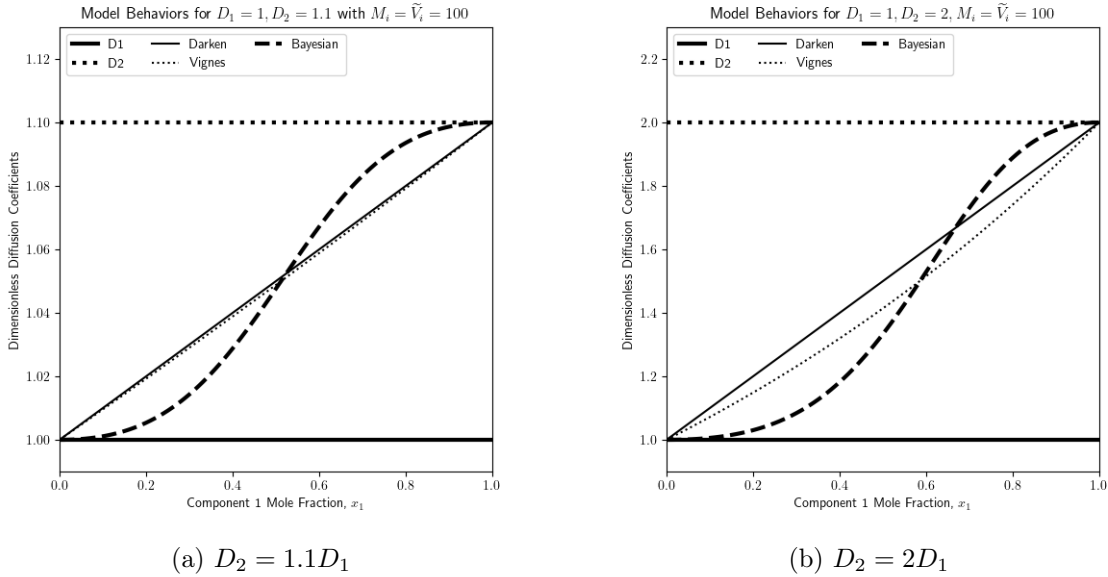


Figure 1: Binary model behaviors for  $\mathcal{D}$  with varying  $D_2/D_1$ .

In Figure 1(b), the self-diffusion coefficient of component 2 is increased to double that of component 1. As the difference in self-diffusion coefficients gets bigger, the deviations of the Vignes and Bayesian coefficients from the Darken values grow in both magnitude and, in the Bayesian case, asymmetry about the center of the concentration range. The Vignes deviations are one-sided, while the Bayesian model deviates to both sides of the Darken values. The Bayesian model deviates below the Darken values over a fraction of the concentration range in approximate proportion to the ratio of the greater to lesser self-diffusion coefficients and above the Darken values over the remaining concentration range.

In the first two cases, we varied the self-diffusion coefficients independently of the molar volumes, but some relationship between the two is expected. Fig. 2 shows the results when the molar volume of the second component is set so that the ratio of component self-diffusion coefficients is inversely proportional to the ratio of component molar volumes. In this case, the sigmoidal behavior of the Bayesian model disappears and the Bayesian values coincide with the Darken values.

In fact, one can show algebraically that, when the ratio of the self-diffusion coefficients is equal to the inverse ratio of molar volumes:

$$\frac{D_2}{D_1} = \frac{\tilde{V}_1}{\tilde{V}_2}, \quad (47)$$

the Bayesian and Darken models are equivalent. The ratio in Eq. (47) also arises when Bearman's [6] friction-based theory is applied to regular solutions. In that case, Bearman's theory results in an MS diffusion coefficient,  $\mathcal{D}$ , that takes the Darken form.

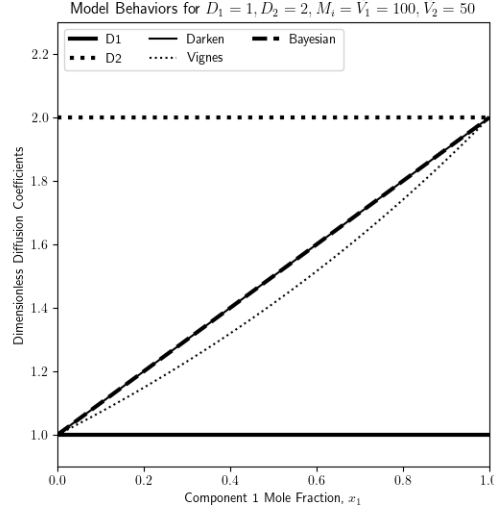


Figure 2: Binary model behaviors for  $\mathcal{D}$  with  $D_1/D_2 = \tilde{V}_2/\tilde{V}_1$ .

The results above do not consider associations between component molecules. To gain insight into the effects of such associations, we start with a generalized Darken form based on Carman's [8] model where clusters may form in either component:

$$\mathcal{D} = x_1 f_2 D_2 + x_2 f_1 D_1 \quad (48)$$

The  $f_i$  are composition dependent functions included to account for clustering of component  $i$ . For example, Moggridge [35] uses a fixed  $f_1 = 2$  to represent dimerization of the alcohols in solutions of methanol or ethanol with carbon tetrachloride. For the mutual diffusion coefficients to approach their appropriate pure component limits, must have:

$$\lim_{x_2 \rightarrow 1} f_1 = 1, \quad \lim_{x_1 \rightarrow 1} f_2 = 1 \quad (49)$$

It is clear that as a general weighted function, Eq. (48) could be used to fit any continuous functional representation of  $\mathcal{D}$  given continuous functional representations of the component self-diffusion coefficients. To retain their physical significance as adjustments for intra-species clustering, the  $f_i$  must take values equal to or greater than 1. Given that constraint, it is instructive to see how the cluster weighting functions impact  $\mathcal{D}$ , if only for comparison with the Bayesian model results discussed below.

To model a function that obeys the required limits and is broadly active over the concentration range, let  $f_i$  take the form:

$$\begin{aligned} f_i &= 1 + f \\ f &= f'_i (4x_1 x_2)^{0.25} \end{aligned} \quad (50)$$

Figure 3 shows the cluster model results when  $f'$  ranges from 0 to 1, covering the range from monomers to dimers for component 1 in Fig. 3a and for component 2 in Fig. 3b. The mole fraction weighting of the cluster factor results in increasing enhancement of  $\mathcal{D}$  as the concentration of the non-clustering component increases up to the point where  $f$  decays as it approaches the pure component limits.

The inclusion of an explicit cluster size coefficient is a strong constraint on the modeled process, scaling the corresponding self-diffusion coefficient directly. The correlation coefficient in the self-diffusion covariance matrix of the Bayesian model is an alternative approach to account for component interactions. Figure 4 shows the behavior of the model system where we use the expression for  $f$  in Eq. (50) to represent the concentration dependence of the correlation coefficient,  $r_{12}$ , with  $f'$  spanning the range from  $-0.2$  to  $0.2$ . Negative correlations between species lead to positive deviations from the Darken form, except near the pure component limits, where the deviations become negative. Positive correlations lead to negative deviations from the Darken form that are more broadly distributed relative to the positive deviations at equivalent negative correlation values.

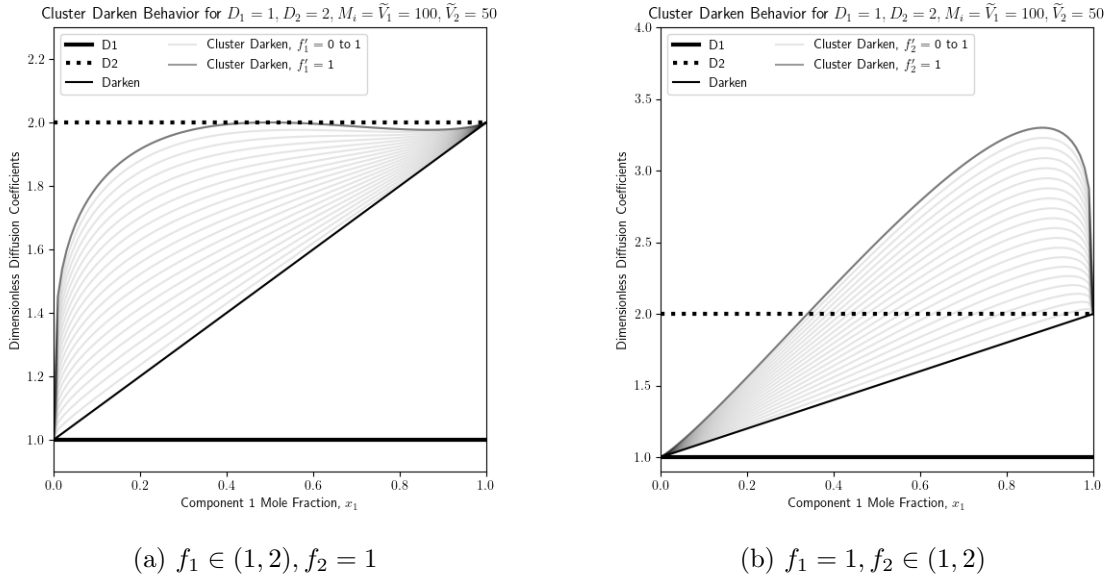


Figure 3: Behavior of cluster Darken model, Eq. (48), with varying cluster coefficients.

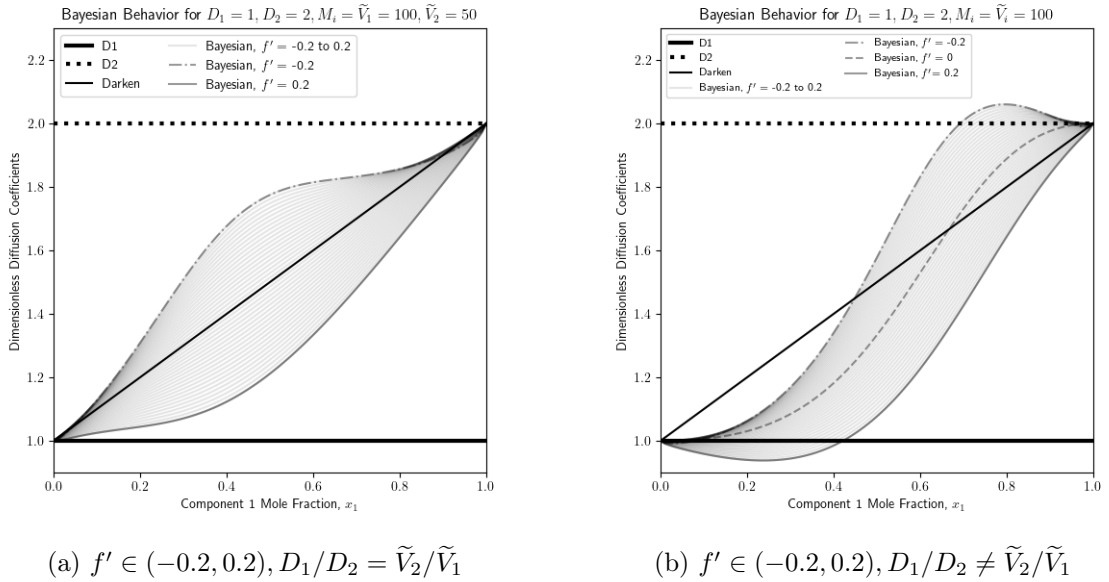


Figure 4: Behavior of Bayesian model, Eq. (44), with varying correlations.

The case studies above make clear that the clustering and correlation functions,  $f_i$  and  $r_{12}$ , considered as general fitting functions, could be used to shape the predicted  $\mathfrak{D}$  over a broad spectrum of behavior. The Bayesian model is distinct in its ability to account for negative deviations from the Darken form when inter-species correlations are positive. The clustering model, on the other hand, allows for stronger positive deviations from the Darken form than are available to the Bayesian model given the range of allowable correlation coefficients. Neither the cluster function nor the correlation function is commonly determined experimentally. Using them as fitting functions may, however, provide insights into the observed mutual diffusion behavior of specific systems.

#### 4.1.3. Comparison with Published Binary Diffusion Data

Moggridge [2012b] presented an extensive comparison between experimental data, the Darken equation, and his thermodynamically adjusted model:

$$D = (x_1 D_2 + x_2 D_1) \Gamma^\alpha \quad (51)$$

Here, we consider a subset of those binary systems where the measured mutual diffusion data show both positive and negative deviations from the Darken predictions, with varying degrees of expected cluster behavior. In each case, we performed a least-squares fit of the published self- and mutual diffusion data using polynomial finite element basis functions [14] such that the pure component limits of the mutual diffusion function match the appropriate self-diffusion limits. The thermodynamic factor,  $\Gamma$ , for each system was computed using Wilson’s model [53] for the activity coefficients with parameters from the DECHEMA vapor-liquid equilibrium data collection [17]. Physical parameters for all components are given in Table 1. Wilson parameters for all systems are given in Table 2. The Wilson parameters for diethyl ether and chloroform are based on vapor-liquid equilibrium data measured at 333 K but were applied in analysis after scaling to 298 K, in agreement with the diffusion data.

Table 1: Component physical properties [21].

Component	Molecular Weight ( $g/mol$ )	Density ( $g/cm^3$ )
Acetone	58.079	0.7845
Benzene	78.112	0.8765
Chloroform	119.378	1.4788
Cyclohexane	84.159	0.7739
Diethyl Ether	74.121	0.7138
n-Hexane	86.175	0.6606
Water	18.015	0.997

Table 2: Binary systems Wilson parameters [17].

System	T (K)	$A_{12}$	$A_{21}$
Cyclohexane - Benzene	298	133.751	170.4476
n-Hexane - Benzene	298	237.6292	225.595
Acetone - Benzene	298	418.0568	-104.7155
Acetone - Water	298	-35.189	1468.9208
Acetone - Chloroform	298	-61.812	-431.5877
Diethyl Ether - Chloroform	333	-172.3024	-285.9477
Diethyl Ether - Chloroform, temperature adjusted	298	-154.2007	-255.9067

For each system, we present three figures. In the first, we compare experimental data to mutual diffusion coefficients computed from: the Darken model, Eq. (51), with  $\alpha = 1$ ; Moggridge’s [36] thermodynamically modified Darken form, Eq. (51) with  $\alpha = 0.64$ ; the Bayesian model, Eq. (44), with the correlation function,  $r_{12}$ , set to zero; and the Bayesian model, Eq. (44), with a fitted correlation function. For several systems, we also show fitted cluster models based on Eq. (48) with an unmodified  $\Gamma$ . Following Moggridge [36], we show the published mutual diffusion coefficient data as points for comparison. Published self-diffusion coefficients are also shown as point values together with their associated finite element basis function fit. The fitted self-diffusion polynomials are used to compute the various model mutual diffusion coefficients across the concentration range. The first figure is also shaded below the real root limits, Eq. (45) and Eq. (46), for the mutual diffusion coefficients. Real roots can not be found when the mutual diffusion coefficient fit is above this region. The second figure for each system shows the fitted self-diffusion coefficients together with various model MS diffusion coefficients,  $\mathcal{D}$ , and a functional representation of  $\mathcal{D}$  generated by dividing the mutual diffusion data’s finite element basis function fit by the thermodynamic factor  $\Gamma$ . The third figure shows the correlation function,  $r_{12}$ , as regressed from the polynomial fits to the self- and mutual diffusion coefficient data and, where possible, as roots to Eq. (44). For some systems, the figure also includes the cluster function fits from the polynomial fits to the self- and mutual diffusion coefficients. These functions provide some insight into the deviations from ideal behavior that occur in each system. Both the correlation and cluster function fits are forced to zero at the pure component limits.

*Cyclohexane - Benzene.* Self-diffusion coefficients for cyclohexane and benzene at 298 K are from Mills [33] and digitized from Figure 1 in McCall and Anderson [32]. Mutual diffusion coefficients are from Rodwin et al. [43], Sanni et al. [44], and Sanni and Hutchison [45]. For this system, the ratios of self-diffusion coefficients are close to inverse proportion to the ratio of species molar volumes, resulting in ideal ( $r_{12} = 0$ ) Bayesian MS diffusion coefficients that are close to the Darken form. In Figure 5(b), we see that the mutual diffusion fit implied MS diffusion coefficients exhibit positive deviations from ideal behavior, either Darken or Bayesian, over most of the concentration range. Such deviations can be accounted for by shrinking the thermodynamic factor [36], with a small negative correlation coefficient, or by intra-species clustering in either component. For this system, the required correlation correction, shown in Figure 5(c), is a small negative correlation over most of the concentration range. At the low end of the cyclohexane concentration range, the real correlation constraint

Eq. (45) is violated, and only a best fit value can be found. Failure to find a real correlation coefficient at low concentrations appears more likely due to the mis-characterized values of the self- and mutual diffusion coefficients than to the need for an extreme correlation coefficient. We consider this failure further below. Tomza et al. [48] studied clustering behavior in cyclohexane and benzene, reporting evidence of intra-species clusters that reach their maximum concentrations in the pure component limits and inter-species clusters across the concentration range that reach their maximum concentration in the middle of the concentration range, with a 60/40 ratio of intra- and inter-species clusters in the middle of the concentration range.

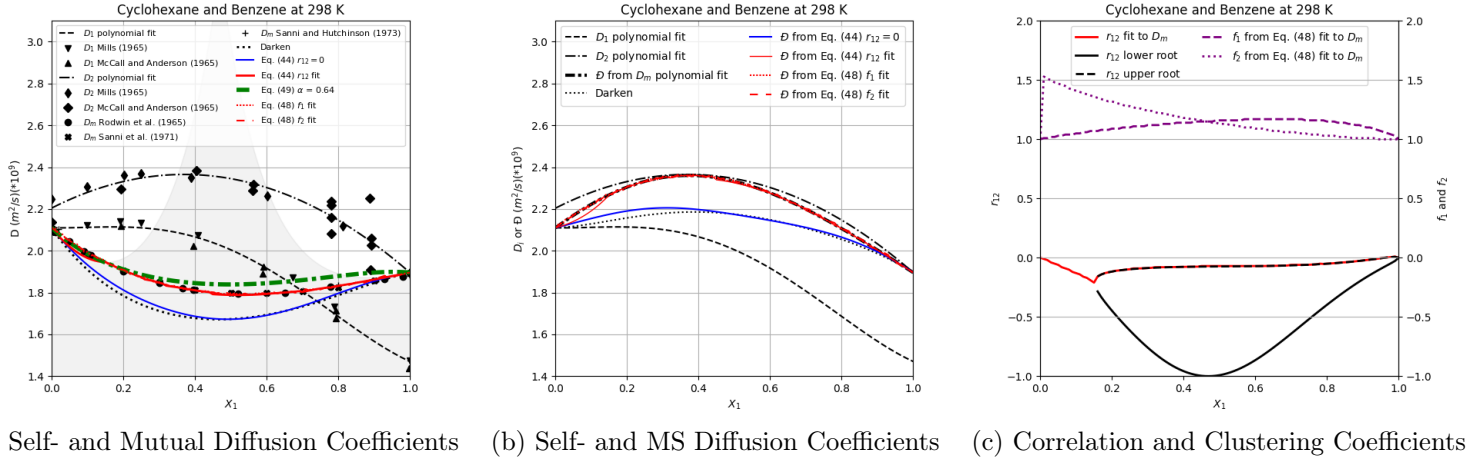
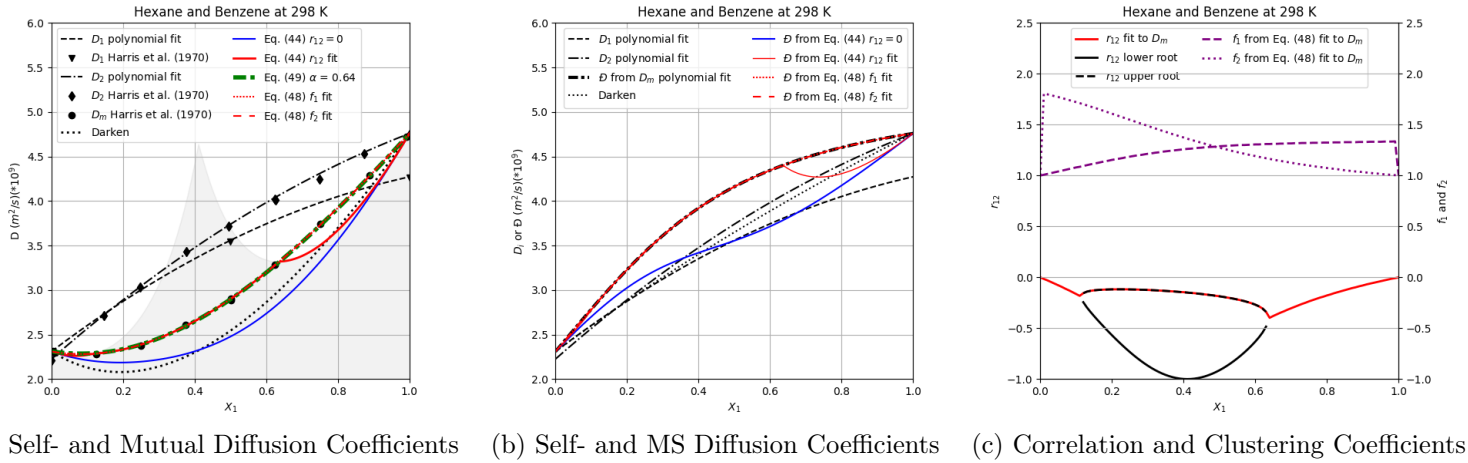


Figure 5: Model behavior for cyclohexane and benzene.

*n-Hexane - Benzene.* Self- and mutual diffusion coefficients for *n*-hexane and benzene at 298 K are from Harris et al. [20]. In this case, the self-diffusion coefficients are further from inverse proportion to the pure component molar volumes, and the ideal Bayesian MS diffusion coefficients display stronger sigmoidal deviation from the Darken coefficients, as described in Section 4.1.2. The mutual diffusion fit implied MS diffusion coefficients show significant positive deviations from the ideal behaviors. These deviations can be accounted for with either Moggridge's adjusted the thermodynamic factor or clustering in either component, but the system violates the real correlation constraints in Eq. (45) and Eq. (46) at the ends of the concentration range. As with cyclohexane and benzene, intra- and inter-species clusters have been observed for this system by Tomza et al. [48], with similar concentration dependence to that described above.

Figure 6: Model behavior for *n*-hexane and benzene.

*Acetone - Benzene.* Self-diffusion coefficients for acetone and benzene at 298 K are from Kamei and Oishi [27]. Mutual diffusion data are from Anderson et al. [4], Cullinan and Toor [10] and Berg et al. [7]. For this system, the ideal Bayesian MS diffusion coefficients are very close to the Darken values. The fitted mutual diffusion coefficient data lead to MS diffusion coefficients that exhibit significant positive deviations from the ideal behaviors. The mutual diffusion coefficients can be fit with Moggridge's thermodynamically adjusted Darken form, Eq. (5), with a slight negative correlation function, or with mild clustering functions on either component. The latter three fits are nearly indistinguishable in Figure 7(a). However, the real correlation constraints, Eq. (45) and Eq. (46), are again violated at the ends of the concentration range, where the fitted

values are the best approximation the model can provide to the mutual diffusion data. These results are consistent with the molecular simulations of acetone and benzene mixtures by Požar et al. [40], who report the tendency of acetone to form dimers.

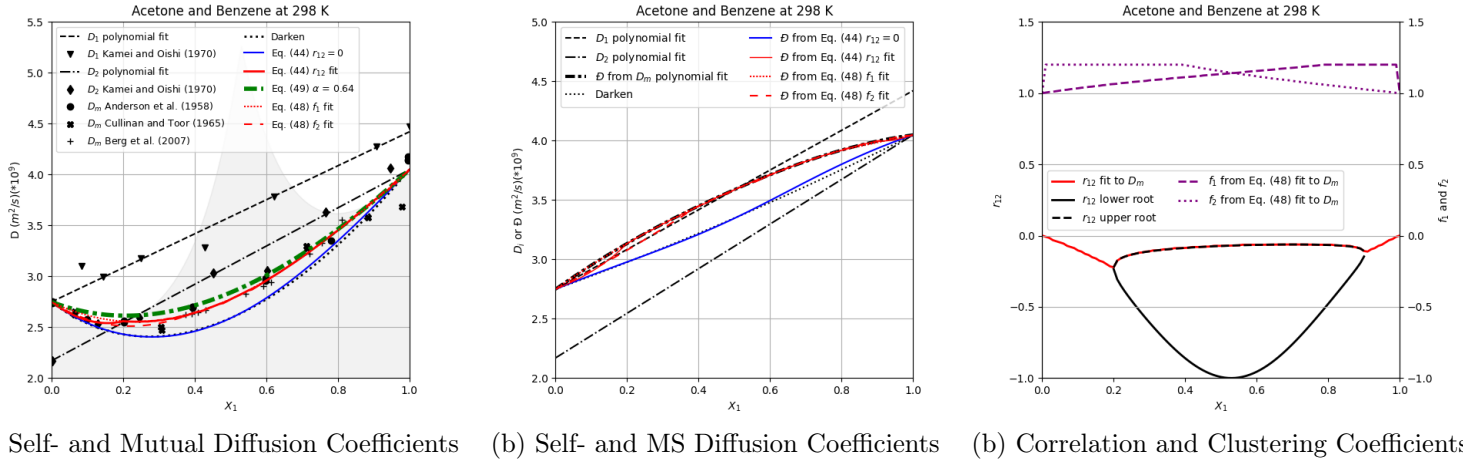


Figure 7: Model behavior for acetone and benzene.

*Acetone - Water.* Self-diffusion coefficients for acetone and water at 298 K are from Kamei and Oishi [27] and Mills and Hertz [34]. Mutual diffusion data are from Anderson et al. [4]. For this system, the molar volume of acetone is roughly four times that of water, yet the self-diffusion coefficients are similar over much of the concentration range. Thus, we see significant deviations between the ideal Bayesian MS diffusion coefficients and the Darken values. The mutual diffusion fit implied MS diffusion coefficients also show significant positive deviations from the ideal behaviors. These mutual diffusion data can be reasonably represented by Moggridge’s thermodynamically adjusted model or with a fitted cluster model, but the Bayesian model fails over all but a very small region at the low end of the concentration range. Strong cluster functions are required to fit the mutual diffusion data. Apicella et al. [5] observed both acetone-rich and water-rich clusters in this system.

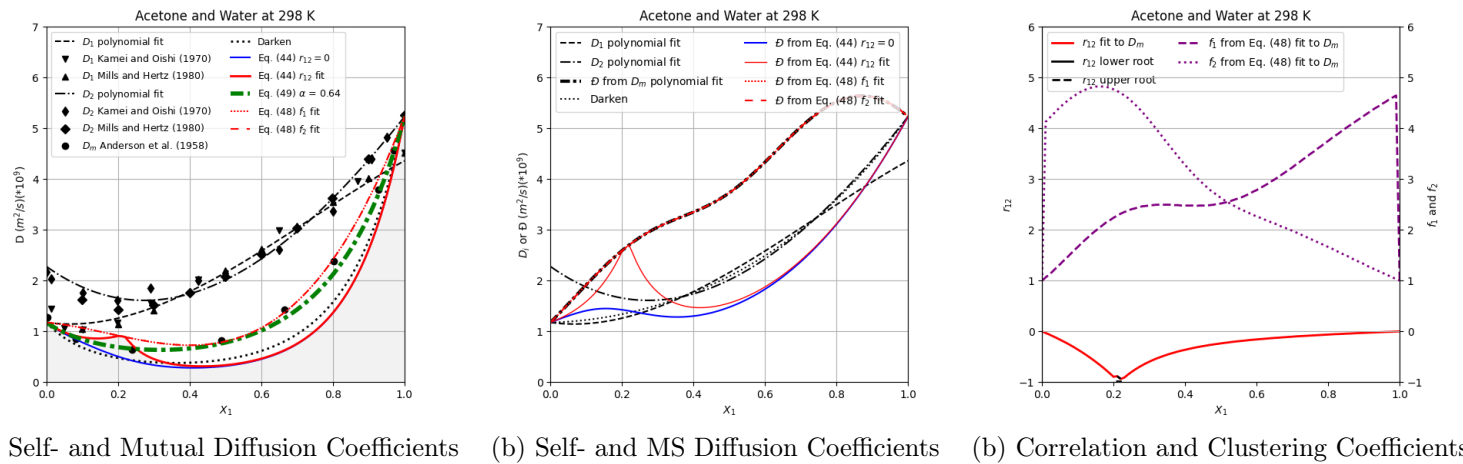
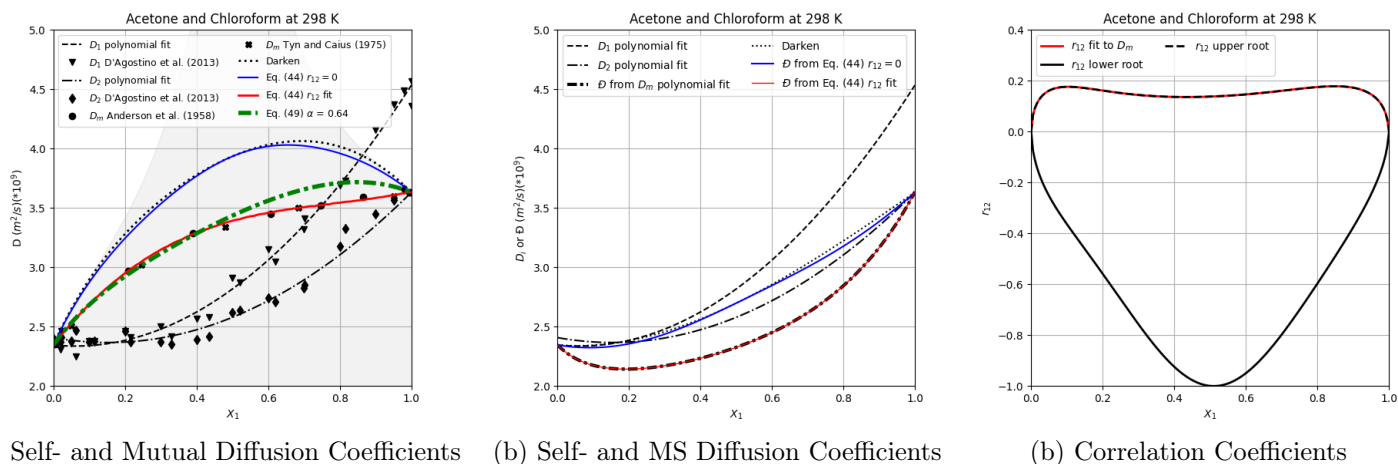


Figure 8: Model behavior for acetone and water.

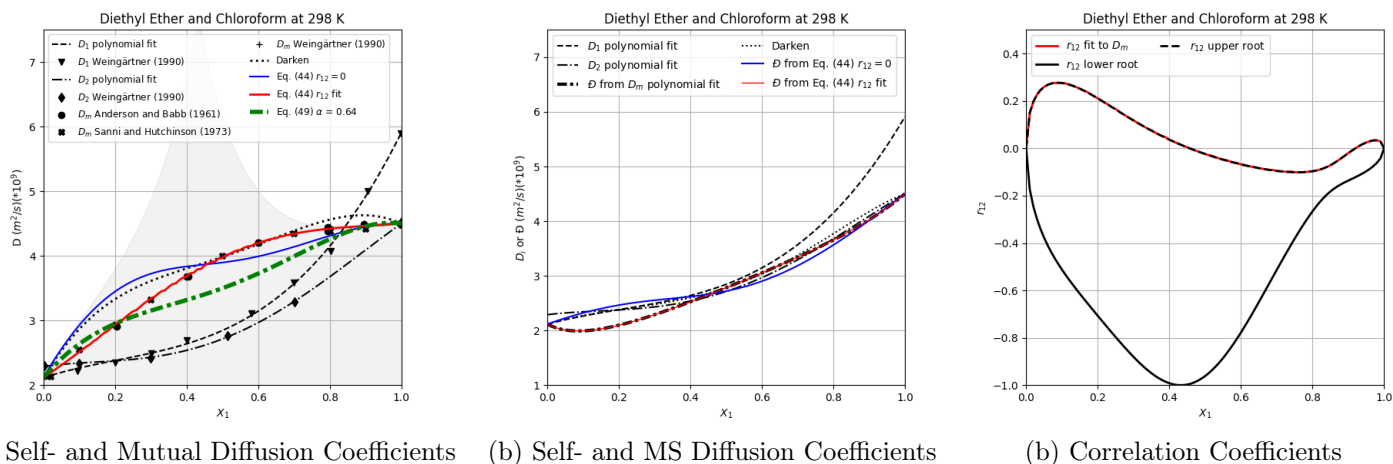
*Acetone - Chloroform.* Self-diffusion coefficients for acetone and chloroform at 298 K are from D’Agostino et al. [12]. Mutual diffusion data are from Anderson et al. [4] and Tyn and Calus [49]. The Darken and ideal Bayesian MS diffusion coefficients for this system are very similar. Unlike the previous systems, the MS diffusion coefficients exhibit significant negative deviations from the ideal behaviors. The upper Bayesian correlation coefficient accounts for the negative deviations from ideality with positive values over the full concentration range, excluding the pure component limits. Such behavior can not be represented by the intra-species cluster model. This correlation structure is consistent with the inter-species associations observed in mixtures of acetone and chloroform reported by Monakhova et al. [37].



(a) Self- and Mutual Diffusion Coefficients (b) Self- and MS Diffusion Coefficients (c) Correlation Coefficients

Figure 9: Model behavior for acetone and chloroform.

*Diethyl Ether - Chloroform.* Self- and mutual diffusion coefficient data for diethyl ether and chloroform at 298 K were digitized from Figure 3 in Weingärtner [52]. Additional mutual diffusion data are from Anderson and Babb [3] and Sanni and Hutchison [45]. The ratio of measured diethyl ether to chloroform self-diffusion coefficients varies significantly over the concentration range, and so the ideal Bayesian model mutual and MS diffusion coefficients shows the expected sigmoidal deviations from the Darken form. The MS diffusion coefficients implied by the polynomial fit to the mutual diffusion data and the Wilson-based  $\Gamma$  show negative deviations from the Darken form at both ends of the concentration range, and slight positive deviations in the middle. These deviations can not be accounted for by intra-species clustering. The Bayesian correlation function fit is positive over roughly the lower half of the diethyl ether concentration range and becomes increasingly negative before rising to slightly positive near the pure diethyl ether limit. Kutsyk et al. [30] report inter-species clusters for this system.



(a) Self- and Mutual Diffusion Coefficients (b) Self- and MS Diffusion Coefficients (c) Correlation Coefficients

Figure 10: Model behavior for diethyl ether and chloroform.

#### 4.1.4. Bayesian Comparisons to Published Data

In the previous section, we took the usual approach to model comparison with experimental data insofar as we compared results based only upon “best fits” to the published diffusion and vapor-liquid equilibrium data. Following this approach, the Bayesian diffusion model yielded, as roots, complete real correlation coefficients across the full concentration range for only two of the six systems considered. Failure in the case of acetone and water was not unexpected, given that system’s highly non-ideal nature. Failure in the other systems was less foreseeable. In this section, we reconsider the systems of cyclohexane and benzene at 298 K and acetone and benzene at 298 K, treating the underlying data and their functional representations in a more complete Bayesian framework. In these cases, we can sample from the posterior distributions for the functional fits of the self- and mutual diffusion coefficients and the activity model parameters to find model parameter sets that yield real correlation coefficients across the full concentration range.

To treat the thermodynamics factor in a Bayesian way, we performed a Bayesian regression on the data provided in the DECHEMA compilations using the Python package Dynesty [46]. The Bayesian regression of the linked polynomial finite

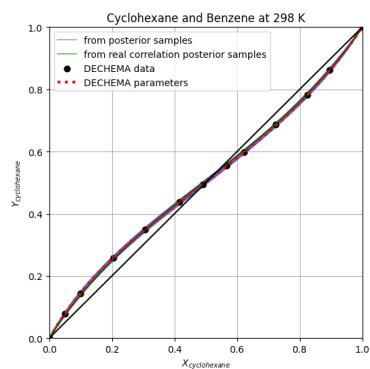
element basis function representations of the self- and mutual diffusion coefficients was also performed using Dynesty. In all cases, uniform priors were defined on the model parameters and on the log of the standard deviations for the Gaussian likelihood functions used in the regressions. Priors were set to allow uncertainty in the fits beyond the standard deviation of errors to the least-squares fits. The objective was to examine whether the Bayesian diffusion model could provide real correlation coefficients over the full concentration range given functional representations of the thermodynamic and diffusion data that were reasonably consistent with the uncertainty in the measured data. These regressions were not meant to yield optimal Bayesian inferences on the model parameters.

For each system, we show five figures. The first figure shows a plot of the vapor-liquid equilibrium data from the DECHEMA compilation together with Wilson-based predictions using samples from the regression posterior, the subset of posterior samples leading to complete real correlations functions, and the original DECHEMA parameters. The second figure is a scatter plot of posterior samples, samples for which the Bayesian diffusion model gave complete real correlation functions, and the original DECHEMA regression values. The third figure is a plot of the self- and mutual diffusion data and polynomial representations based on posterior samples that yield complete real correlations across the concentration range. The fourth figure shows the least-squares self- and MS diffusion coefficient fits and MS diffusion coefficients computed from posterior samples that resulted in complete real correlation functions. The final figure shows the complete real Bayesian model correlation functions computed from the posterior samples for the polynomial self- and mutual diffusion coefficients representations and the Wilson parameters.

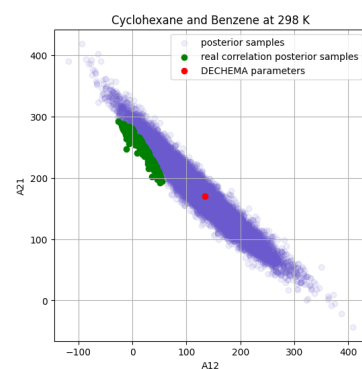
*Cyclohexane - Benzene.* The x-y vapor-equilibrium data for cyclohexane and benzene, shown in Figure 11 (a), are reasonably represented by a broad range of Wilson parameters, shown in Figure 11 (b). The original DECHEMA Wilson parameters are at the center of the posterior distribution, suggesting the Bayesian regression is consistent with the original least-squares procedure. The Wilson parameters leading to complete real correlations in the diffusion model encompass a region of the posterior that is shifted relative to the least-squares result. The mutual diffusion data from multiple sources are consistent, leading to a tight distribution of posterior mutual diffusion curves, shown in Figure 11 (c). There is greater uncertainty in the component self-diffusion coefficients. We find that the self-diffusion coefficients leading to complete real correlations are evenly spread about the least-squares fits. The shifted Wilson parameters corresponding complete real correlation functions lead to significantly shifted MS diffusion coefficients relative to the least-squares MS diffusion coefficients, as shown in green in Figure 11(d). The resultant real correlation curves, shown in Figure 11 (e), are concentrated in a region between -0.06 and 0.05, with rising values at both ends of the concentration range. As noted above, Tomza et al. [48] studied clustering behavior in cyclohexane and benzene, reporting evidence of intra-species clusters that reach their maximum concentrations in the pure component limits and inter-species clusters across the concentration range that reach their maximum concentration in the middle of the concentration range. The real correlation functions suggest both types of clustering: positive regions at both ends correspond to negative deviations from ideal behavior, either Darken or Bayesian, i.e., the presence of inter-species clusters, and negative values over the central concentration region correspond to positive deviations from the ideal MS diffusion coefficients, indicating the presence of intra-species clusters. The shape of the correlation functions, however, appear reversed to Tomza et al.'s observed cluster concentration profiles. These differences raise the question as to what extent of any intra- or inter-species clustering is embedded in the measured self-diffusion data. If that is the case, the Bayesian model correlation function may be serving as a correction to the data rather than a full, independent accounting of the system's clustering behavior. It is also not clear how the net impact of coexisting intra- and inter-species clustering should manifest in the correlation function. Overall, these results indicate the sensitivity of the model's implied diffusive correlation structure due to uncertainty in the characterizations of thermodynamic and diffusion data. This is not surprising given Alabi-Babalola et al.'s [1] recent demonstration of the sensitivity of other diffusion model fits to the choice of thermodynamic model.

*Acetone - Benzene .* For acetone and benzene, the VLE data, shown in Figure 12 (a), are reasonably represented by the broad range of Wilson parameters, shown in Figure 12 (b), present in the Bayesian regression posterior. The DECHEMA Wilson parameters again appear near the center of the Bayesian posterior, indicating consistency with the DECHEMA least-squares results. The Wilson parameters leading to real correlation coefficients lie directly adjacent to the DECHEMA parameters. There is greater uncertainty in the characterizations of the mutual diffusion behavior for this system relative to that of cyclohexane and benzene, as seen in Figure 12 (c). The acetone self-diffusion samples that lead to real correlations are biased above the least-squares fit, while those for benzene are more evenly distributed around the least-squares result. The MS diffusion coefficients implied by the posterior samples, shown in Figure 12 (d), show predominantly negative deviations from ideal behavior, in marked contrast to the least-squares implied values, which show positive deviations from ideal behavior. The posterior sampled real correlations are predominantly positive though small, generally less than 0.05 across the concentration range, suggesting some degree of inter-species association. This appears to be inconsistent with the molecular simulations of acetone and benzene mixtures of Požar et al. [40], who report the tendency of acetone to form dimers but no inter-species clusters.

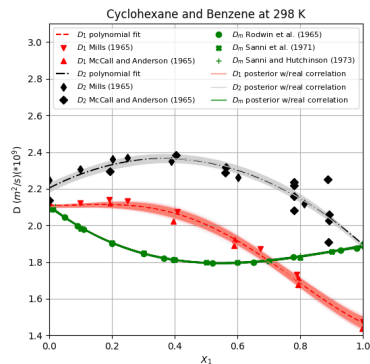




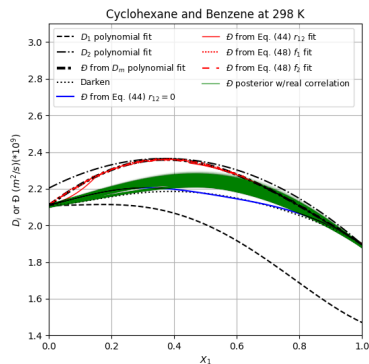
(a) VLE Data and Wilson Predictions



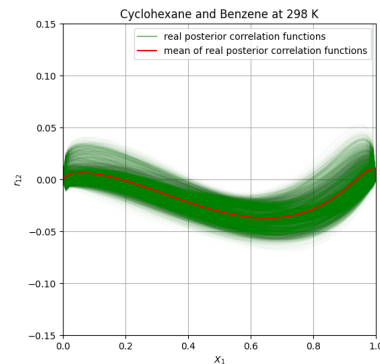
(b) Wilson Parameters



(c) Self- and Mutual Diffusion Coefficients

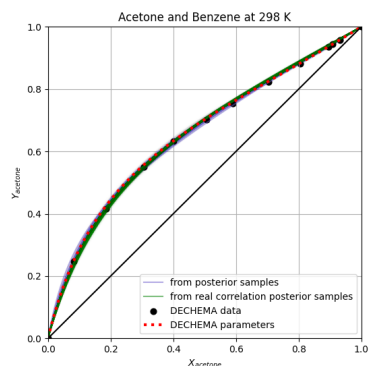


(d) Self- and MS Diffusion Coefficients

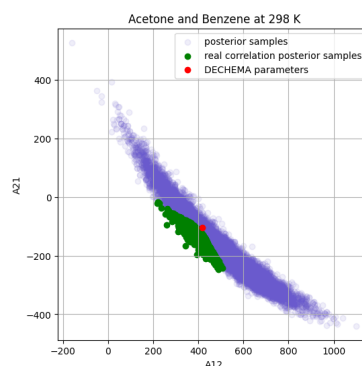


(e) Correlation Coefficients

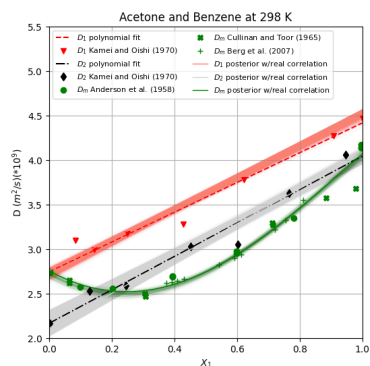
Figure 11: Posterior views for cyclohexane and benzene.



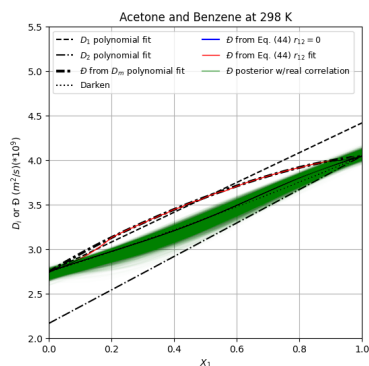
(a) VLE Data and Wilson Predictions



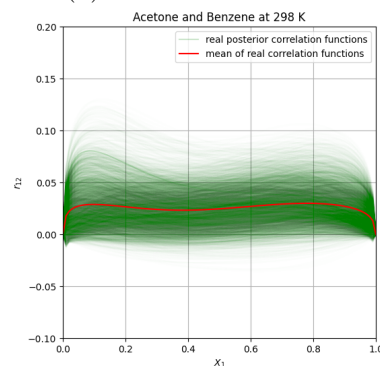
(b) Wilson Parameters



(c) Self- and Mutual Diffusion Coefficients



(d) Self- and MS Diffusion Coefficients



(e) Correlation Coefficients

Figure 12: Posterior views for acetone and benzene.

*Other Systems*. Similar analysis of the systems n-hexane and benzene, and acetone and water, failed to yield real correlation coefficients in the Bayesian diffusion model across the full concentration range. Both of these systems required stronger clustering functions to fit their mutual diffusion data. While the model can provide a physically reasonable description of four of the six systems considered, lack of complete characterizations for these two systems suggests the need for further prior knowledge in construction of a model that can represent the full range of potential correlation and cluster behavior.

#### 4.1.5. Correlations from Local Compositions

Local composition-based activity models have found widespread success in thermodynamic applications [28]. As noted earlier, a number of authors [31, 54, 55] have reported improvements in diffusion model predictions when local compositions are substituted for bulk compositions. Since local compositions differ from bulk compositions as a result of intermolecular associations, they may provide a starting point for *a priori* estimates of the Bayesian model correlation function for some systems. If we assume that the inter-species local mole fractions in positive excess of the corresponding bulk value represent associations that move with correlation 1, and those in negative excess to the bulk value represent associations that move with correlation -1, we can posit that a weighted blend of those excess values represents the average inter-species correlation:

$$r_{12} = x_1 (x_{21} - x_2) + x_2 (x_{12} - x_1) \quad (52)$$

where  $x_{21}$  represents the local mole fraction of component 2 around a molecule of component 1, and  $x_{12}$  represents the local mole fraction of component 1 around a molecule of component 2. For the Wilson model, these are given by the expressions:

$$x_{21} = \frac{x_2 \Lambda_{21}}{x_1 + x_2 \Lambda_{21}}, \quad x_{12} = \frac{x_1 \Lambda_{12}}{x_1 \Lambda_{12} + x_2} \quad (53)$$

$\Lambda_{12}$  and  $\Lambda_{21}$  are given by:

$$\Lambda_{21} = \frac{\tilde{V}_1}{\tilde{V}_2} \exp\left(-\frac{A_{21}}{RT}\right), \quad \Lambda_{12} = \frac{\tilde{V}_2}{\tilde{V}_1} \exp\left(-\frac{A_{12}}{RT}\right) \quad (54)$$

where  $A_{12}$  and  $A_{21}$  are the Wilson parameters, as listed in Table 2 and shown in Figures 11 and 12 for the present systems of interest.

*Cyclohexane and Benzene*. Figure 13 (a) shows the Bayesian model predictions for the mutual diffusion coefficients in the systems of cyclohexane and benzene at 298 K based on samples from the Bayesian regression posteriors for this system's self-diffusion coefficients and Wilson parameters. Figure 13 (b) shows the local composition-based correlation functions, Eq. (52), based on the posterior samples of the Wilson parameters used to compute the results in Figure 13 (a). The means of the sampled results are also shown. We find that the mean of the sample predictions for the mutual diffusion coefficients is in reasonable agreement with the measured data, but the local-composition correlations are somewhat different than the real correlation functions shown in Figure 11 (e). The local composition-based correlations, almost entirely negative over the full concentration range, are consistent with the intra-species clustering observed by Tomza et al. [48], but fail to indicate the inter-species clustering that they observed reaching maximum concentration at the center of the concentration range. The results may, however, simply reflect the net impact of both types of clusters.

*Acetone and Benzene*. Figure 14 (a) shows the Bayesian model predictions, and corresponding mean, for the mutual diffusion coefficients in the systems of acetone and benzene at 298 K based on samples from the Bayesian regression posteriors for this system's self-diffusion coefficients and Wilson parameters. Figure 14 (b) shows the local composition-based correlation functions, and corresponding mean, based on the posterior samples of the Wilson parameters used to compute the results in Figure 14 (a). We find that the mean of the sample predictions for the mutual diffusion coefficients is again in reasonable agreement with the measured data, but for this system, the local-composition correlations show the opposite sign over most of the concentration range relative to the real correlation functions shown in Figure 12 (e). Regions of negative correlation functions computed with the local composition-based form, Eq. (52), suggest intra-species association and are consistent with the acetone dimerization observed in molecular simulations by Požar et al. [40].

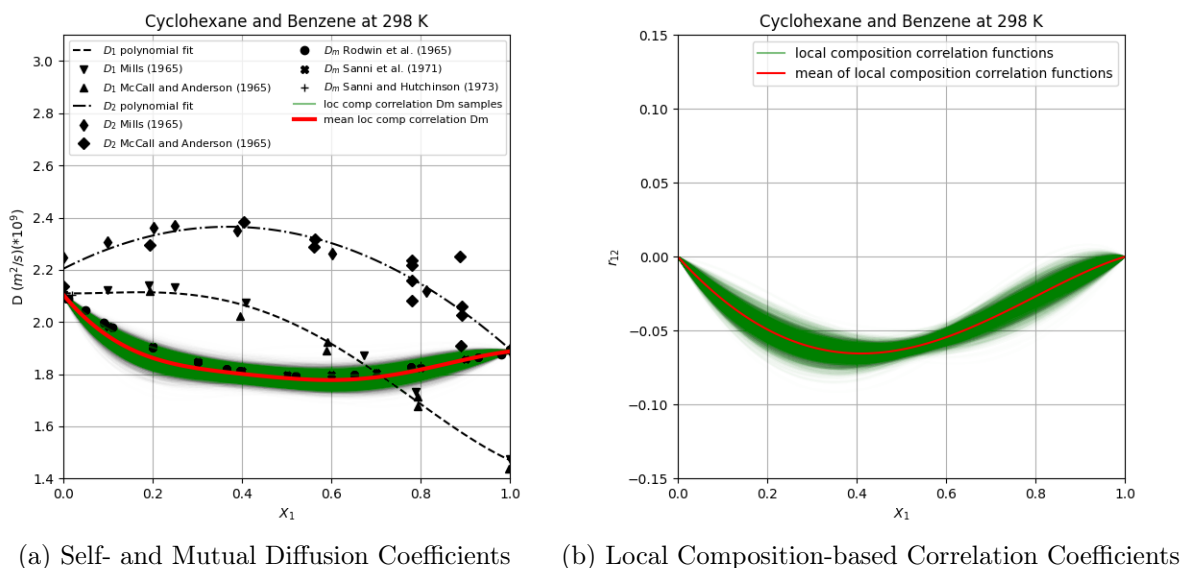


Figure 13: Local-composition based results for cyclohexane and benzene.

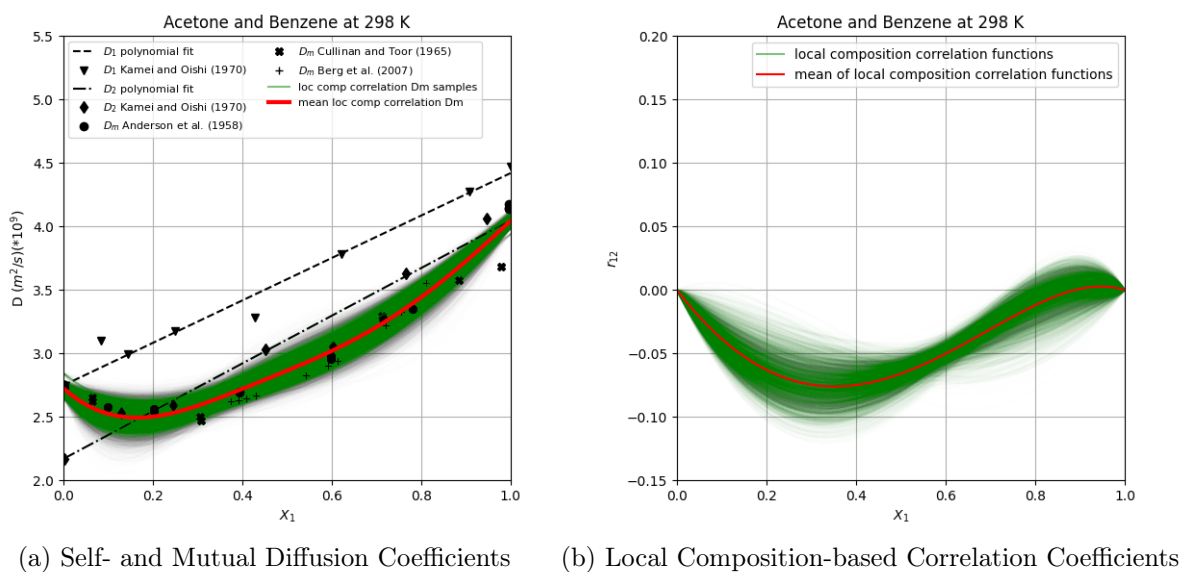


Figure 14: Local-composition based results for acetone and benzene.

*Other Systems.* A predictive form for the correlation function realizes the objective of a theory that can predict mutual diffusion coefficients from self-diffusion coefficients and an activity model. Applications of the thermodynamically adjusted Darken model, Eq. (5), by Moggridge, D'Agostino and their collaborators [35, 1] have been remarkably successful, but scaling of the thermodynamic term in systems far from their consolute points blurs the theoretical distinction between the inter-species frictions and the fundamental concept that the force driving diffusive motion is the gradient in chemical potential. Though derived on an information theoretic basis, the Bayesian theory retains the separation of these concepts. In application, we are hopeful that the local composition-based correlation function will provide reasonable estimates of mutual diffusion behavior for mildly non-ideal systems. As the intermolecular associations become stronger and more complex, it is likely to fail, as we have observed but not presented for the system of diethyl ether and chloroform at 298 K. More broadly, it is not clear if any of the available local composition-based activity models can be expected to be consistent with observed clustering behavior, even on a net intra- and inter-species cluster basis. Predictive forms for the correlation function clearly warrant further development, but evaluations of such forms will have to account for uncertainty in functional characterizations of self-diffusion and thermodynamic parameters, which, as the results above indicate, certainly impact perceived success of the model for any given system.

## 4.2. Multicomponent Systems

Extension of the Bayesian diffusion model to multicomponent systems requires only some additional algebra. We start by writing the joint probability distribution for the past positions of the molecules of each species presently at the position of interest, which we take to be the origin of our chosen reference frame:

$$P(\mathbf{z} \mid \mathbf{x} = 0, \tau, I) = A_5 \left( \prod_{i=1}^N a_i(z_i) \right) \exp \left[ -\frac{\mathbf{z}^T \boldsymbol{\Sigma}^{-1} \mathbf{z}}{2} \right] \quad (55)$$

where  $A_5$  is the normalizing constant, and:

$$\boldsymbol{\Sigma} = \begin{bmatrix} \tau D_1 & \tau r_{12} \sqrt{D_1 D_2} & \cdots & \tau r_{1N} \sqrt{D_1 D_N} \\ \tau r_{12} \sqrt{D_1 D_2} & \tau D_2 & \cdots & \vdots \\ \vdots & \vdots & \ddots & \tau r_{N-1N} \sqrt{D_{N-1} D_N} \\ \tau r_{1N} \sqrt{D_1 D_N} & \cdots & \tau r_{N-1N} \sqrt{D_{N-1} D_N} & \tau D_N \end{bmatrix}, \quad (56)$$

$$\mathbf{z} = \begin{bmatrix} z_1 \\ \vdots \\ z_N \end{bmatrix}$$

As before, we set the derivative with respect to  $\mathbf{z}$  of the logarithm of Eq. (55) equal to zero to find the optimal past position of the components and include additional prior information on the component motions consistent with our chosen reference frame and the Gibbs-Duhem equation. The former gives  $z_N$  in terms of the other  $z_i$ . The latter constrains the  $N^{\text{th}}$  component log-activity gradients in terms of the gradients of the other component log-activities. To solve the resultant system of equations, we factor out the log-activity gradients and assume them locally constant over the range spanning the individual  $z_i$ .

A full examination of the multicomponent theory is beyond the scope of the present paper, however, as an illustrative example, consider the molar flux with respect to the volume average velocity. Taking the logarithm of Eq. (55) gives:

$$\ln(P(\mathbf{z} \mid \mathbf{x} = 0, \tau, I)) = \ln(A_5) + \sum_{i=1}^N (\ln(a_i(z_i))) - \frac{\mathbf{z}^T \boldsymbol{\Sigma}^{-1} \mathbf{z}}{2} \quad (57)$$

Differentiating with respect to  $z_i$  and imposing the flux and Gibbs-Duhem constraints yields, for  $i$  from 1 to  $N-1$ :

$$\frac{d \ln(a_i(z_i))}{dz_i} + \frac{d \ln(a_N(z_N))}{dz_N} \frac{dz_N}{dz_i} - \mathbf{f}_i^T \boldsymbol{\Sigma}^{-1} \mathbf{z}' = \frac{d \ln(a_i)}{dz_i} - \sum_{j=1}^{N-1} \left( \frac{\phi_i \phi_j \tilde{V}_N}{\phi_N^2 \tilde{V}_j} \frac{d \ln(a_j)}{dz_i} \right) - \mathbf{f}_i^T \boldsymbol{\Sigma}^{-1} \mathbf{z}' = 0 \quad (58)$$

where:

$$\mathbf{f}_i = \begin{bmatrix} \delta_{ij} \\ \vdots \\ \delta_{ij} \\ -\frac{\phi_i}{\phi_N} \end{bmatrix}, \quad \mathbf{z} = \begin{bmatrix} z_1 \\ \vdots \\ z_N \end{bmatrix} \quad (59)$$

and  $j$  indicates the row number in  $\mathbf{f}_i$ , i.e.,  $\delta_{ij} = 0$  for all but the  $i^{\text{th}}$  row, where  $j = i$ , of  $\mathbf{f}_i$ . This set of equations can be cast in matrix form and solved for the vector of optimal past positions,  $\hat{\mathbf{z}}$ :

$$\hat{\mathbf{z}} = \boldsymbol{\Lambda}^{-1} \boldsymbol{\Phi} \boldsymbol{\alpha} \quad (60)$$

where:

$$\hat{\mathbf{z}} = \begin{bmatrix} \hat{z}_1 \\ \vdots \\ \hat{z}_{N-1} \end{bmatrix}, \quad \boldsymbol{\Lambda} = \mathbf{F}^T \boldsymbol{\Sigma}^{-1} \mathbf{F}, \quad \mathbf{F} = \begin{bmatrix} 1 & 0 & \cdots & 0 \\ 0 & 1 & 0 & \vdots \\ \vdots & 0 & \ddots & 0 \\ 0 & \cdots & 0 & 1 \\ -\frac{\phi_1}{\phi_N} & -\frac{\phi_2}{\phi_N} & \cdots & -\frac{\phi_{N-1}}{\phi_N} \end{bmatrix} \quad (61)$$

and:

$$\Phi = \begin{bmatrix} 1 + \frac{\phi_1^2 \tilde{V}_N}{\phi_N^2 \tilde{V}_1} & \frac{\phi_1 \phi_2 \tilde{V}_N}{\phi_N^2 \tilde{V}_2} & \dots & \frac{\phi_1 \phi_{N-1} \tilde{V}_N}{\phi_N^2 \tilde{V}_{N-1}} \\ \frac{\phi_2 \phi_1 \tilde{V}_N}{\phi_N^2 \tilde{V}_1} & 1 + \frac{\phi_2^2 \tilde{V}_N}{\phi_N^2 \tilde{V}_2} & \frac{\phi_2 \phi_3 \tilde{V}_N}{\phi_N^2 \tilde{V}_3} & \vdots \\ \vdots & \frac{\phi_3 \phi_2 \tilde{V}_N}{\phi_N^2 \tilde{V}_2} & \ddots & \frac{\phi_{N-2} \phi_{N-1} \tilde{V}_N}{\phi_N^2 \tilde{V}_{N-1}} \\ \frac{\phi_{N-1} \phi_1 \tilde{V}_N}{\phi_N^2 \tilde{V}_1} & \dots & \frac{\phi_{N-1} \phi_{N-2} \tilde{V}_N}{\phi_N^2 \tilde{V}_{N-2}} & 1 + \frac{\phi_{N-1}^2 \tilde{V}_N}{\phi_N^2 \tilde{V}_{N-1}} \end{bmatrix}, \quad \alpha = \begin{bmatrix} \frac{d \ln(a_1)}{dz} \\ \vdots \\ \frac{d \ln(a_{N-1})}{dz} \end{bmatrix} \quad (62)$$

#### 4.2.1. Ideal Ternary Systems

For the case of a ternary system where the self-diffusive correlations are all zero, solving for  $\hat{z}_1$  and  $\hat{z}_2$  gives:

$$\begin{bmatrix} \hat{z}_1 \\ \hat{z}_2 \end{bmatrix} = \frac{2\tau}{\sum_{i=1}^N \phi_i^2 D_i} \begin{bmatrix} D_1 \left( \phi_2^2 D_2 + \left( \phi_1^2 \frac{\tilde{V}_3}{\tilde{V}_1} + \phi_3^2 \right) D_3 \right) & \phi_1 \phi_2 D_1 \left( \frac{\tilde{V}_3}{\tilde{V}_2} D_3 - D_2 \right) \\ \phi_2 \phi_1 D_2 \left( \frac{\tilde{V}_3}{\tilde{V}_1} D_3 - D_1 \right) & D_2 \left( \phi_1^2 D_1 + \left( \phi_2^2 \frac{\tilde{V}_3}{\tilde{V}_2} + \phi_3^2 \right) D_3 \right) \end{bmatrix} \begin{bmatrix} \frac{d \ln(a_1)}{dz} \\ \frac{d \ln(a_2)}{dz} \end{bmatrix} \quad (63)$$

The component flux expressions are:

$$J_i^V = C_i (\hat{v}_i - v^V) = C_i \frac{-z_i}{2\tau} \quad (64)$$

yielding:

$$\begin{bmatrix} J_1^V \\ J_2^V \end{bmatrix} = \frac{-1}{\sum_{i=1}^N \phi_i^2 D_i} \begin{bmatrix} C_1 D_1 \left( \phi_2^2 D_2 + \left( \phi_1^2 \frac{\tilde{V}_3}{\tilde{V}_1} + \phi_3^2 \right) D_3 \right) & C_1 \phi_1 \phi_2 D_1 \left( \frac{\tilde{V}_3}{\tilde{V}_2} D_3 - D_2 \right) \\ C_2 \phi_2 \phi_1 D_2 \left( \frac{\tilde{V}_3}{\tilde{V}_1} D_3 - D_1 \right) & C_2 D_2 \left( \phi_1^2 D_1 + \left( \phi_2^2 \frac{\tilde{V}_3}{\tilde{V}_2} + \phi_3^2 \right) D_3 \right) \end{bmatrix} \begin{bmatrix} \frac{d \ln(a_1)}{dz} \\ \frac{d \ln(a_2)}{dz} \end{bmatrix} \quad (65)$$

To cast the result in the usual multicomponent Fickian form:

$$J_i^V = - \sum_{j=1}^{N-1} D_{ij} \frac{\partial C_j}{\partial z}, \quad (66)$$

we expand the activity gradients in the component concentrations. For a ternary system, we have:

$$\begin{bmatrix} \frac{d \ln(a_1)}{dz} \\ \frac{d \ln(a_2)}{dz} \end{bmatrix} = \begin{bmatrix} \frac{d \ln(a_1)}{dC_1} & \frac{d \ln(a_1)}{dC_2} \\ \frac{d \ln(a_2)}{dC_1} & \frac{d \ln(a_2)}{dC_2} \end{bmatrix} \begin{bmatrix} \frac{dC_1}{dz} \\ \frac{dC_2}{dz} \end{bmatrix} \quad (67)$$

Grouping terms results in the following main and cross-term mutual diffusion coefficients:

$$\begin{aligned} D_{11} &= \frac{D_1}{\sum_{i=1}^3 \phi_i^2 D_i} \left\{ \left( \phi_2^2 D_2 + \left( \phi_1^2 \frac{\tilde{V}_3}{\tilde{V}_1} + \phi_3^2 \right) D_3 \right) \frac{d \ln(a_1)}{d \ln(C_1)} + \phi_1 \phi_2 \left( \frac{\tilde{V}_3}{\tilde{V}_2} D_3 - D_2 \right) \frac{d \ln(a_2)}{d \ln(C_1)} \right\} \\ D_{12} &= \frac{D_1}{\sum_{i=1}^3 \phi_i^2 D_i} \left\{ \left( \phi_2^2 D_2 + \left( \phi_1^2 \frac{\tilde{V}_3}{\tilde{V}_1} + \phi_3^2 \right) D_3 \right) C_1 \frac{d \ln(a_1)}{dC_2} + \phi_1 \phi_2 \left( \frac{\tilde{V}_3}{\tilde{V}_2} D_3 - D_2 \right) C_1 \frac{d \ln(a_2)}{dC_2} \right\} \\ D_{21} &= \frac{D_2}{\sum_{i=1}^3 \phi_i^2 D_i} \left\{ \phi_2 \phi_1 \left( \frac{\tilde{V}_3}{\tilde{V}_1} D_3 - D_1 \right) C_2 \frac{d \ln(a_1)}{dC_1} + \left( \phi_1^2 D_1 + \left( \phi_2^2 \frac{\tilde{V}_3}{\tilde{V}_2} + \phi_3^2 \right) D_3 \right) C_2 \frac{d \ln(a_2)}{dC_1} \right\} \\ D_{22} &= \frac{D_2}{\sum_{i=1}^3 \phi_i^2 D_i} \left\{ \phi_2 \phi_1 \left( \frac{\tilde{V}_3}{\tilde{V}_1} D_3 - D_1 \right) \frac{d \ln(a_1)}{d \ln(C_2)} + \left( \phi_1^2 D_1 + \left( \phi_2^2 \frac{\tilde{V}_3}{\tilde{V}_2} + \phi_3^2 \right) D_3 \right) \frac{d \ln(a_2)}{d \ln(C_2)} \right\} \end{aligned} \quad (68)$$

With the help of the Gibbs-Duhem equation, we find that when the correlation coefficients are zero and the self-diffusion coefficients scale inversely with the component molar volumes, the Bayesian model mutual diffusion coefficients match those of the multicomponent Darken form, expressed here as derived from Bearman's friction-based approach in Price and Romdhane [41]:

$$D_{ik} = C_i \sum_{j=1, j \neq i}^N \phi_j \left( D_i \frac{d \ln(a_i)}{dC_k} - D_j \frac{d \ln(a_j)}{dC_k} \right) \quad (69)$$

Both main and cross diffusion coefficients also go to their correct dilute solution limits. Further investigation of the Bayesian model in the multicomponent context will be the subject of future research.

## 5. Conclusion

This paper presents several extensions of Jaynes' [24] derivation of Fick's Law from Bayes' Theorem. The simplest extensions include multiple components, alternative reference frames, and a change in the prior probability term to reflect a driving force based on chemical potentials rather than concentrations. These extensions are based on information about individual components in the system, yielding model forms that have been widely used in applications to solvent-polymer systems. The next extension is based on joint inference of molecular motions of both components in a binary system. The unique element of this extension is its inclusion of a composition dependent correlation coefficient that can account for both positive and negative deviations of the MS diffusion coefficients from ideal, i.e., independent, behavior, owing to negative and positive, respectively, correlation between the species self-diffusive motions. In the limit where the ratio of component self-diffusion coefficients are inversely proportional to their molar volumes, the model MS diffusion coefficients equal the Darken values. When that ratio does not hold, but inter-species correlations are zero, the model provides a broader definition of ideal behavior. Comparison of model fits to experimental data indicate that the Bayesian model is capable of providing accurate correlations of mutual diffusion behavior. While the theory provides no prescription for computing the correlation function based on system characteristics, we provide a possible starting point based on local compositions and hope that having this new model relating self- and mutual-diffusion coefficients might spur further efforts to characterize the correlation behavior, both theoretical and experimental. We do find that the correlation function can not account for observed behavior when strong clustering occurs. In that sense, the model delineates systems where a more complete description of clustering across the concentration range is required. The final extension presents the model in its full multicomponent form and the special case of an ideal, i.e., independent species self-diffusive motions, ternary system. Again, the Bayesian expressions for the ternary mutual diffusion coefficients collapse to a multicomponent form of the Darken equation when the ratios of self-diffusion coefficients are inversely proportional to the component molar volumes, indicating that the Bayesian model is a generalization of the Darken model.

## Acknowledgment

An earlier, less complete, and erroneous version of the present study was developed while the author was employed in the Corporate Research Process Laboratory at 3M, with 3M having granted permission to publish and present on those results. The author would like to acknowledge the encouragement of the late Prof. L. E. Scriven to pursue development of that then incomplete theory. His words of support were a welcomed boost at a time when such were nowhere else forthcoming.

---

## References

- [1] Alabi-Babalola, O., Zhong, J., Moggridge, G.D., D'Agostino, C., 2024. Rationalizing the use of mutual diffusion prediction models in non-ideal binary mixtures. *Chemical Engineering Science* 291, 119930. URL: <https://www.sciencedirect.com/science/article/pii/S0009250924002306>, doi:<https://doi.org/10.1016/j.ces.2024.119930>.
- [2] Alsoy, S., Duda, J.L., 1999. Modeling of multicomponent drying of polymer films. *AIChE Journal* 45, 896–905. URL: <http://doi.wiley.com/10.1002/aic.690450420>, doi:10.1002/aic.690450420.
- [3] Anderson, D.K., Babb, A.L., 1961. Mutual Diffusion in Non-Ideal Liquid Mixtures. II. Diethyl Ether—Chloroform. *The Journal of Physical Chemistry* 65, 1281–1283. URL: <https://doi.org/10.1021/j100826a001>, doi:10.1021/j100826a001. *eprint*: <https://doi.org/10.1021/j100826a001>.
- [4] Anderson, D.K., Hall, J.R., Babb, A.L., 1958. Mutual Diffusion in Non-ideal Binary Liquid Mixtures. *The Journal of Physical Chemistry* 62, 404–408. URL: <https://pubs.acs.org/doi/abs/10.1021/j150562a006>, doi:10.1021/j150562a006.
- [5] Apicella, B., Li, X., Passaro, M., Russo, C., 2016. Insights on Clusters Formation Mechanism by Time of Flight Mass Spectrometry. 2. The Case of Acetone–Water Clusters. *Journal of the American Society for Mass Spectrometry* 27, 1835–1845. URL: <https://pubs.acs.org/doi/10.1007/s13361-016-1464-3>, doi:10.1007/s13361-016-1464-3.
- [6] Bearman, R.J., 1961. On The Molecular Basis of Some Current Theories of Diffusion <sup>1</sup>. *The Journal of Physical Chemistry* 65, 1961–1968. URL: <https://pubs.acs.org/doi/abs/10.1021/j100828a012>, doi:10.1021/j100828a012.
- [7] Berg, R.W., Hansen, S.B., Shapiro, A.A., Stenby, E.H., 2007. Diffusion Measurements in Binary Liquid Mixtures by Raman Spectroscopy. *Applied Spectroscopy* 61, 367–373. URL: <http://journals.sagepub.com/doi/10.1366/000370207780466316>, doi:10.1366/000370207780466316.

- [8] Carman, P.C., 1967. Self-diffusion and interdiffusion in complex-forming binary systems. *The Journal of Physical Chemistry* 71, 2565–2572. URL: <https://pubs.acs.org/doi/abs/10.1021/j100867a027>, doi:10.1021/j100867a027.
- [9] Caticha, A., 2007. Information and Entropy. *AIP Conference Proceedings* 954, 11–22. URL: <http://arxiv.org/abs/0710.1068>, doi:10.1063/1.2821253. arXiv: 0710.1068.
- [10] Cullinan, H.T., Toor, H.L., 1965. Diffusion in the Three-Component Liquid System Acetone-Benzene-Carbon Tetrachloride. *The Journal of Physical Chemistry* 69, 3941–3949. URL: <https://pubs.acs.org/doi/abs/10.1021/j100895a050>, doi:10.1021/j100895a050.
- [11] D’Agostino, C., Mantle, M.D., Gladden, L.F., Moggridge, G.D., 2011. Prediction of binary diffusion coefficients in non-ideal mixtures from NMR data: Hexane–nitrobenzene near its consolute point. *Chemical Engineering Science* 66, 3898–3906. URL: <https://www.sciencedirect.com/science/article/pii/S0009250911003150>, doi:<https://doi.org/10.1016/j.ces.2011.05.014>.
- [12] D’Agostino, C., Stephens, J., Parkinson, J., Mantle, M., Gladden, L., Moggridge, G., 2013. Prediction of the mutual diffusivity in acetone–chloroform liquid mixtures from the tracer diffusion coefficients. *Chemical Engineering Science* 95, 43–47. URL: <https://linkinghub.elsevier.com/retrieve/pii/S0009250913002157>, doi:10.1016/j.ces.2013.03.033.
- [13] Darken, L.S., 1948. Diffusion, mobility and their interrelation through free energy in binary metallic systems. *Trans. AIME* 175, 184–201.
- [14] Dhatt, G., Touzot, G., 1984. *The Finite Element Method Displayed*. Wiley.
- [15] Einstein, A., Fürth, R., Cowper, A.D., 1956. *Investigations on the theory of brownian movement*. Dover, New York.
- [16] Fick, A., 1995. On liquid diffusion. *Journal of Membrane Science* 100, 33–38. URL: <https://linkinghub.elsevier.com/retrieve/pii/037673889400230V>, doi:10.1016/0376-7388(94)00230-V.
- [17] Gmehling, J., Onken, U., Arlt, W., 1993. *Vapour-liquid equilibrium data collection*. Dechema.
- [18] Guevara-Carrion, G., Janzen, T., Muñoz-Muñoz, Y.M., Vrabec, J., 2016. Mutual diffusion of binary liquid mixtures containing methanol, ethanol, acetone, benzene, cyclohexane, toluene, and carbon tetrachloride. *The Journal of Chemical Physics* 144, 124501. URL: <http://aip.scitation.org/doi/10.1063/1.4943395>, doi:10.1063/1.4943395.
- [19] Haase, R.R., 1990. *Thermodynamics of Irreversible Processes*. Dover.
- [20] Harris, K.R., Pua, C.K.N., Dunlop, P.J., 1970. Mutual and tracer diffusion coefficients and frictional coefficients for the systems benzene-chlorobenzene, benzene-n-hexane, and benzene-n-heptane at 25.deg. *The Journal of Physical Chemistry* 74, 3518–3529. URL: <https://pubs.acs.org/doi/abs/10.1021/j100713a015>, doi:10.1021/j100713a015.
- [21] Haynes, W.M., Lide, D.R., Bruno, T.J. (Eds.), 2016. *CRC Handbook of Chemistry and Physics*. 97th ed., CRC Press.
- [22] Howie, D., 2002. *Interpreting probability: controversies and developments in the early twentieth century*. Cambridge studies in probability, induction, and decision theory, Cambridge University Press, Cambridge New York.
- [23] Hsu, Y.D., Chen, Y.P., 1998. Correlation of the mutual diffusion coefficients of binary liquid mixtures. *Fluid Phase Equilibria* 152, 149–168. URL: <https://linkinghub.elsevier.com/retrieve/pii/S0378381298003756>, doi:10.1016/S0378-3812(98)00375-6.
- [24] Jaynes, E.T., 1989. Clearing up mysteries—the original goal, in: *Maximum Entropy and Bayesian Methods*: Cambridge, England, 1988. Springer, pp. 1–27.
- [25] Jaynes, E.T., Bretthorst, G.L., 2003. *Probability theory: the logic of science*. Cambridge university press, Cambridge.
- [26] Jianmin, Y., Shenglong, L., Xianjin, L., 2008. Phenomenological Models of Diffusivities Based on Local Composition. *Advances in Natural Science* 1, 24–38. URL: <http://www.cscanada.net/index.php/ans/article/view/j.ans.1715787020080101.004.004/36>.
- [27] Kamei, Y., Oishi, Y., 1970. Self-Diffusion Coefficients of Water and Acetone in Water-Acetone System. Issue: 4 Pages: 403 Publication Title: *Nippon Kagaku Zasshi* Volume: 91.
- [28] Kontogeorgis, G., Folas, G., 2010. Activity Coefficient Models Part 2: Local Composition Models, from Wilson and NRTL to UNIQUAC and UNIFAC, in: *Thermodynamic Models for Industrial Applications*. John Wiley & Sons, Ltd, pp. 109–157. URL: <https://onlinelibrary.wiley.com/doi/abs/10.1002/9780470747537.ch5>, doi:<https://doi.org/10.1002/9780470747537.ch5>.

- [29] Krishna, R., 2015. Uphill diffusion in multicomponent mixtures. *Chemical Society Reviews* 44, 2812–2836. URL: <http://xlink.rsc.org/?DOI=C4CS00440J>, doi:10.1039/C4CS00440J.
- [30] Kutsyk, A.M., Ilchenko, O.O., Nikonova, V.V., Obukhovskiy, V.V., 2021. Mixing dynamics of diethyl ether and chloroform. *Journal of Molecular Liquids* 339, 116687. URL: <https://www.sciencedirect.com/science/article/pii/S0167732221014112>, doi:<https://doi.org/10.1016/j.molliq.2021.116687>.
- [31] Li, J., Liu, H., Hu, Y., 2001. A mutual-diffusion-coefficient model based on local composition. *Fluid Phase Equilibria* 187–188, 193–208. URL: <https://linkinghub.elsevier.com/retrieve/pii/S0378381201005350>, doi:10.1016/S0378-3812(01)00535-0.
- [32] McCall, D.W., Anderson, E.W., 1966. Self-Diffusion in Cyclohexane-Benzene Solutions. *The Journal of Physical Chemistry* 70, 601–602. URL: <http://pubs.acs.org/doi/abs/10.1021/j100874a514>, doi:10.1021/j100874a514.
- [33] Mills, R., 1965. The Intradiffusion<sup>1,2</sup> and Derived Frictional Coefficients for Benzene and Cyclohexane in Their Mixtures at 25°. *The Journal of Physical Chemistry* 69, 3116–3119. URL: <https://pubs.acs.org/doi/abs/10.1021/j100893a051>, doi:10.1021/j100893a051.
- [34] Mills, R., Hertz, H.G., 1980. Application of the velocity cross-correlation method to binary nonelectrolyte mixtures. *The Journal of Physical Chemistry* 84, 220–224. URL: <https://api.semanticscholar.org/CorpusID:95866746>.
- [35] Moggridge, G., 2012a. Prediction of the mutual diffusivity in binary liquid mixtures containing one dimerising species, from the tracer diffusion coefficients. *Chemical Engineering Science* 76, 199–205. URL: <https://linkinghub.elsevier.com/retrieve/pii/S0009250912002400>, doi:10.1016/j.ces.2012.04.014.
- [36] Moggridge, G., 2012b. Prediction of the mutual diffusivity in binary non-ideal liquid mixtures from the tracer diffusion coefficients. *Chemical Engineering Science* 71, 226–238. URL: <https://linkinghub.elsevier.com/retrieve/pii/S0009250911008724>, doi:10.1016/j.ces.2011.12.016.
- [37] Monakhova, Y.B., Pozharov, M.V., Zakharova, T.V., Khvorostova, E.K., Markin, A.V., Lachenmeier, D.W., Kuballa, T., Mushtakova, S.P., 2014. Association/Hydrogen Bonding of Acetone in Polar and Non-polar Solvents: NMR and NIR Spectroscopic Investigations with Chemometrics. *Journal of Solution Chemistry* 43, 1963–1980. URL: <http://link.springer.com/10.1007/s10953-014-0249-1>, doi:10.1007/s10953-014-0249-1.
- [38] Nauman, E.B., Savoca, J., 2001. An engineering approach to an unsolved problem in multicomponent diffusion. *AIChE Journal* 47, 1016–1021. URL: <http://doi.wiley.com/10.1002/aic.690470508>, doi:10.1002/aic.690470508.
- [39] Obukhovskiy, V.V., Kutsyk, A.M., Nikonova, V.V., Ilchenko, O.O., 2017. Nonlinear diffusion in multicomponent liquid solutions. *Physical Review E* 95. URL: <https://link.aps.org/doi/10.1103/PhysRevE.95.022133>, doi:10.1103/PhysRevE.95.022133.
- [40] Požar, M., Segulier, J.B., Guerche, J., Mazighi, R., Zoranić, L., Mijaković, M., Kežić-Lovrinčević, B., Sokolić, F., Perera, A., 2015. Simple and complex disorder in binary mixtures with benzene as a common solvent. *Physical Chemistry Chemical Physics* 17, 9885–9898. URL: <http://xlink.rsc.org/?DOI=C4CP05970K>, doi:10.1039/C4CP05970K.
- [41] Price, P.E., Romdhane, I.H., 2003. Multicomponent diffusion theory and its applications to polymer-solvent systems. *AIChE Journal* 49, 309–322. URL: <http://doi.wiley.com/10.1002/aic.690490204>, doi:10.1002/aic.690490204.
- [42] Renon, H., Prausnitz, J.M., 1968. Local compositions in thermodynamic excess functions for liquid mixtures. *AIChE Journal* 14, 135–144. URL: <https://aiche.onlinelibrary.wiley.com/doi/abs/10.1002/aic.690140124>, doi:<https://doi.org/10.1002/aic.690140124>. [\\_eprint: https://aiche.onlinelibrary.wiley.com/doi/pdf/10.1002/aic.690140124](https://aiche.onlinelibrary.wiley.com/doi/pdf/10.1002/aic.690140124).
- [43] Rodwin, L., Harpst, J.A., Lyons, P.A., 1965. Diffusion in the System Cyclohexane—Benzene. *The Journal of Physical Chemistry* 69, 2783–2785. URL: <http://pubs.acs.org/doi/abs/10.1021/j100892a503>, doi:10.1021/j100892a503.
- [44] Sanni, S.A., Fell, C.J.D., Hutchison, H.P., 1971. Diffusion coefficients and densities for binary organic liquid mixtures. *Journal of Chemical & Engineering Data* 16, 424–427. URL: <https://pubs.acs.org/doi/abs/10.1021/jc60051a009>, doi:10.1021/jc60051a009.
- [45] Sanni, S.A., Hutchison, P., 1973. Diffusivities and densities for binary liquid mixtures. *Journal of Chemical & Engineering Data* 18, 317–322. URL: <http://pubs.acs.org/doi/abs/10.1021/jc60058a028>, doi:10.1021/jc60058a028.
- [46] Speagle, J.S., 2020. dynesty: A Dynamic Nested Sampling Package for Estimating Bayesian Posteriors and Evidences. *Monthly Notices of the Royal Astronomical Society* 493, 3132–3158. URL: <http://arxiv.org/abs/1904.02180>, doi:10.1093/mnras/staa278. arXiv: 1904.02180.



- [47] Taylor, R., Krishna, R., 1993. Multicomponent mass transfer. Wiley series in chemical engineering, Wiley, New York.
- [48] Tomza, P., Wrzeszcz, W., Czarnecki, M.A., 2019. Tracking small heterogeneity in binary mixtures of aliphatic and aromatic hydrocarbons: NIR spectroscopic, 2DCOS and MCR-ALS studies. *Journal of Molecular Liquids* 276, 947–953. URL: <https://www.sciencedirect.com/science/article/pii/S0167732218348827>, doi:<https://doi.org/10.1016/j.molliq.2018.12.131>.
- [49] Tyn, M.T., Calus, W.F., 1975. Temperature and concentration dependence of mutual diffusion coefficients of some binary liquid systems. *Journal of Chemical & Engineering Data* 20, 310–316. URL: <https://pubs.acs.org/doi/abs/10.1021/je60066a009>, doi:10.1021/je60066a009.
- [50] Vignes, A., 1966. Diffusion in Binary Solutions. Variation of Diffusion Coefficient with Composition. *Industrial & Engineering Chemistry Fundamentals* 5, 189–199. URL: <https://pubs.acs.org/doi/abs/10.1021/i160018a007>, doi:10.1021/i160018a007.
- [51] Vrentas, J.S., Vrentas, C.M., 2007. Restrictions on Friction Coefficients for Binary and Ternary Diffusion. *Industrial & Engineering Chemistry Research* 46, 3422–3428. URL: <https://pubs.acs.org/doi/10.1021/ie061593a>, doi:10.1021/ie061593a.
- [52] Weingärtner, H., 1990. The Microscopic Basis of Self Diffusion - Mutual Diffusion Relationships in Binary Liquid Mixtures. *Berichte der Bunsengesellschaft für physikalische Chemie* 94, 358–364. URL: <http://doi.wiley.com/10.1002/bbpc.19900940331>, doi:10.1002/bbpc.19900940331.
- [53] Wilson, G.M., 1964. Vapor-Liquid Equilibrium. XI. A New Expression for the Excess Free Energy of Mixing. *Journal of the American Chemical Society* 86, 127–130. URL: <http://pubs.acs.org/doi/abs/10.1021/ja01056a002>, doi:10.1021/ja01056a002.
- [54] Zhou, M., Yuan, X., Zhang, Y., Yu, K.T., 2013. Local Composition Based Maxwell–Stefan Diffusivity Model for Binary Liquid Systems. *Industrial & Engineering Chemistry Research* 52, 10845–10852. URL: <http://pubs.acs.org/doi/10.1021/ie4010157>, doi:10.1021/ie4010157.
- [55] Zhu, Q., Moggridge, G.D., D’Agostino, C., 2015. A local composition model for the prediction of mutual diffusion coefficients in binary liquid mixtures from tracer diffusion coefficients. *Chemical Engineering Science* 132, 250–258. URL: <https://linkinghub.elsevier.com/retrieve/pii/S0009250915002821>, doi:10.1016/j.ces.2015.04.021.
- [56] Zielinski, J.M., Hanley, B.F., 1999. Practical friction-based approach to modeling multicomponent diffusion. *AIChE Journal* 45, 1–12. URL: <http://doi.wiley.com/10.1002/aic.690450102>, doi:10.1002/aic.690450102.